

Annual Review of Biomedical Engineering
**Micromechanobiology:
Focusing on the Cardiac
Cell–Substrate Interface**

Erica A. Castillo,^{1,2} Kerry V. Lane,²
and Beth L. Pruitt^{2,3,4}

¹Department of Mechanical Engineering, Stanford University, Stanford, California 94305, USA; email: ericasti@stanford.edu

²Department of Mechanical Engineering, University of California, Santa Barbara, California 93106, USA; email: klane@ucsb.edu

³Biomolecular Science and Engineering Program, University of California, Santa Barbara, California 93106, USA

⁴Department of Molecular, Cellular and Developmental Biology, University of California, Santa Barbara, California 93117, USA; email: blp@ucsb.edu

Annu. Rev. Biomed. Eng. 2020. 22:257–84

The *Annual Review of Biomedical Engineering* is online at bioeng.annualreviews.org

<https://doi.org/10.1146/annurev-bioeng-092019-034950>

Copyright © 2020 by Annual Reviews.
All rights reserved

Keywords

biointerface, cell–substrate interface, extracellular matrix (ECM), integrins, mechanobiology, cardiomyocytes

Abstract

Engineered, in vitro cardiac cell and tissue systems provide test beds for the study of cardiac development, cellular disease processes, and drug responses in a dish. Much effort has focused on improving the structure and function of engineered cardiomyocytes and heart tissues. However, these parameters depend critically on signaling through the cellular microenvironment in terms of ligand composition, matrix stiffness, and substrate mechanical properties—that is, matrix micromechanobiology. To facilitate improvements to in vitro microenvironment design, we review how cardiomyocytes and their microenvironment change during development and disease in terms of integrin expression and extracellular matrix (ECM) composition. We also discuss strategies used to bind proteins to common mechanobiology platforms and describe important differences in binding strength to the substrate. Finally, we review example biomaterial approaches designed to support and probe cell–ECM interactions of cardiomyocytes in vitro, as well as open questions and challenges.

ANNUAL
REVIEWS **CONNECT**

www.annualreviews.org

- Download figures
- Navigate cited references
- Keyword search
- Explore related articles
- Share via email or social media

Contents

1. INTRODUCTION	258
2. NATIVE CARDIAC DEVELOPMENT	262
2.1. Temporal Dynamics of Cardiomyocyte Integrin Expression (Development and Disease)	262
2.2. Temporal Dynamics of Myocardial Extracellular Matrix Composition (Development and Disease)	265
3. IN VITRO PROTEIN–SUBSTRATE INTERFACE	271
3.1. Polyacrylamide Hydrogels	271
3.2. Polydimethylsiloxane	272
3.3. Bond Strength of the Linker at the Protein–Substrate Interface	272
4. IN VITRO BIOMATERIALS APPROACHES TO RECAPITULATE THE CARDIOMYOCYTE MICROENVIRONMENT	273
4.1. Ligand Composition	273
4.2. Stiffness	275
4.3. Dimensionality: Two Versus Three Dimensions	275
4.4. Topography	276
5. SUMMARY AND FUTURE DIRECTIONS FOR CONTROLLING THE MICROENVIRONMENT OF CARDIOMYOCYTES VIA BIOMATERIALS ..	276

1. INTRODUCTION

Tissue integrity and cardiac function are achieved by cardiomyocytes (CMs) maintaining cell–extracellular matrix (ECM) and cell–cell interactions (1). Human heart tissue is composed of three layers: endocardium, myocardium, and epicardium (**Figure 1**). The myocardium contracts and relaxes to pump blood throughout the body. Within the myocardium reside CMs, cardiac fibroblasts, cardiac vascular cells, and leukocytes in a network of ECM (**Figure 1**) (2, 3). CMs generate contractile forces and occupy the largest volume fraction of the myocardium (4). Cell subtypes, matrix, and composition differ in the atria, ventricles, and conduction bundles, resulting in varied structural, functional, molecular, and electrophysiological properties (5).

Adherent cell types use various adhesion molecules to physically anchor within this microenvironment (**Figure 2a**) (6). Integrins are the principal receptors that link ECM proteins to the cell cytoskeleton (7, 8). CM integrins serve a wide variety of functions, including adhesion, signaling, viral uptake, ion channel regulation, stem cell differentiation and engraftment, modification of hypertrophic growth responses, and transmission of mechanical signal (mechanotransduction); they may also provide protection from ischemic stress (9). Other nonintegrin ECM receptors (known to interact directly with the ECM) at the cell surface of CMs include the dystroglycan complex and syndecan proteoglycans (10–12). In CMs the structure composed of the dystrophin–glycoprotein complex and the integrin–vinculin–talın complex is known as the costamere (13, 14). In addition to mediating cell–ECM interactions, integrins mediate cell–cell interactions (15). Intercalated discs connect CMs to one another and are composed of adherens junctions, desmosomes, and gap junctions that provide adhesive and electrical coupling between CMs (**Figure 1**) (16). Integrins are bidirectional signal transducers, and ligand binding leads to intracellular signaling events (**Figure 3b**) (17, 18). We use the term outside-in signaling to refer to the cascade of events following integrin–ligand binding. In contrast, inside-out signaling can alter integrin

Cardiomyocytes

(CMs): muscle cells (myocytes) specific to the cardiac (heart) muscle; also known as cardiac myocytes

Extracellular matrix

(ECM): structure composed of water, proteins, and polysaccharides; provides physical structural support to tissues as well as biophysical and biochemical feedback to cells

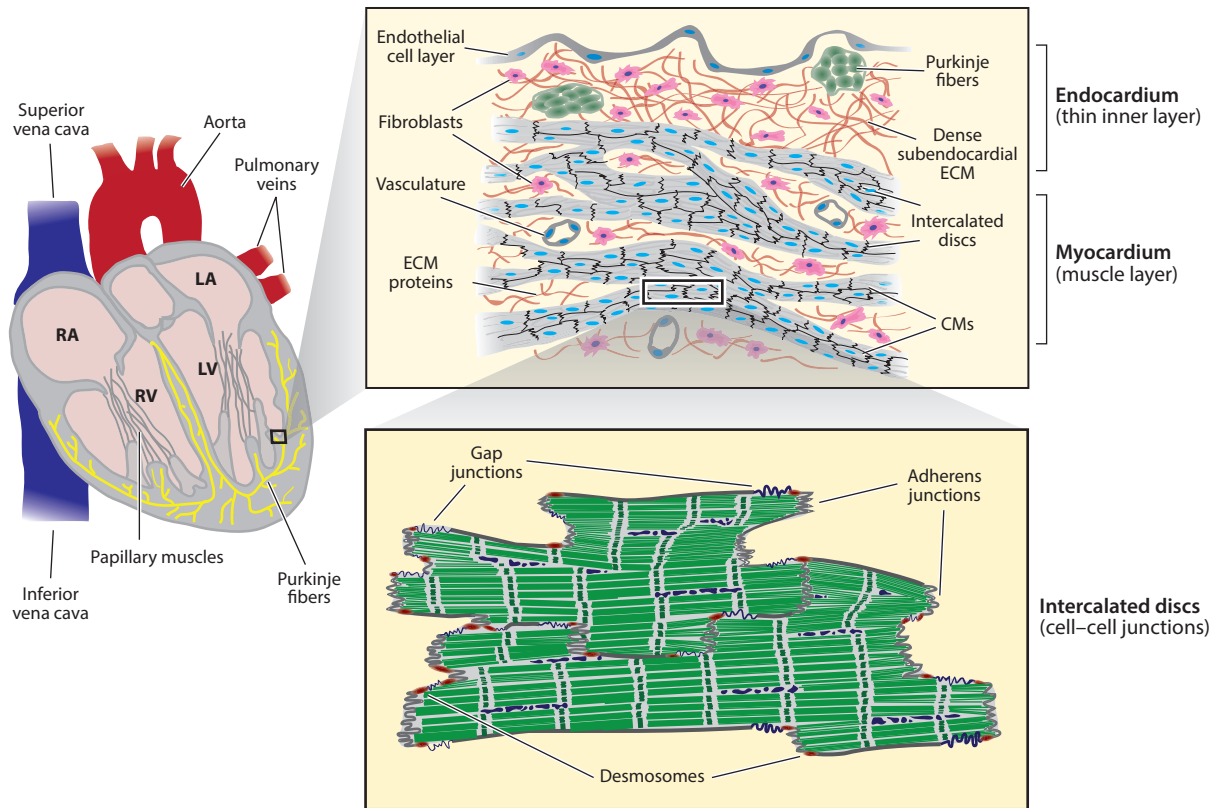


Figure 1

Schematic of the heart and the spatial location of myocardium. The myocardium has a highly ordered, hierarchical structure composed mostly of CMs by volume and mostly fibroblasts by cell number, as well as vascular and other cell types. The cell–ECM and cell–cell junctions provide biophysical and biochemical signals to the CMs. The intercalated discs provide neighboring cells with physical and electrical connections. Abbreviations: CM, cardiomyocytes; ECM, extracellular matrix; LA, left atrium; LV, left ventricle; RA, right atrium; RV, right ventricle. Figure adapted from Reference 3 with permission from The Royal Society of Chemistry.

conformation and binding characteristics from within the cell (17). By simultaneously binding thousands of integrin receptors to ECM binding sites, a cell compiles a spatiotemporal map of the biochemical and biophysical properties of the microenvironment (19).

The heart undergoes constant cycles of contraction and relaxation. Given the dynamic nature of the heart, a robust structural linkage between CMs and extracellular components is needed to transmit forces and deformations (20). The myocardial ECM is composed of glycoproteins (e.g., collagens, elastin, fibronectin, laminin), proteoglycans, glycosaminoglycans, and growth factors (2). The function of each cardiac ECM protein can be structural and/or nonstructural. After being secreted from cells, ECM proteins can undergo further modification and degradation. Matrix metalloproteinases (MMPs) can remodel the matrix and modify the cell–ECM interface (21, 22), while tissue inhibitor metalloproteinases regulate MMP matrix degradation (23). ECM properties such as biochemical composition, mechanical properties, and structure are known to influence CM adhesion and cardiac lineage differentiation, function, and maturity.

CM adhesion receptors and the cardiac microenvironment undergo temporal changes during heart development. Differences in integrin expression profiles are frequently observed in

Costamere: focal adhesion equivalent in striated muscle cells; connects the sarcomeres to the cell membrane, providing robust structural connection to the ECM; composed of two major protein complexes: the integrin–vinculin–talin complex and the dystrophin–glycoprotein complex

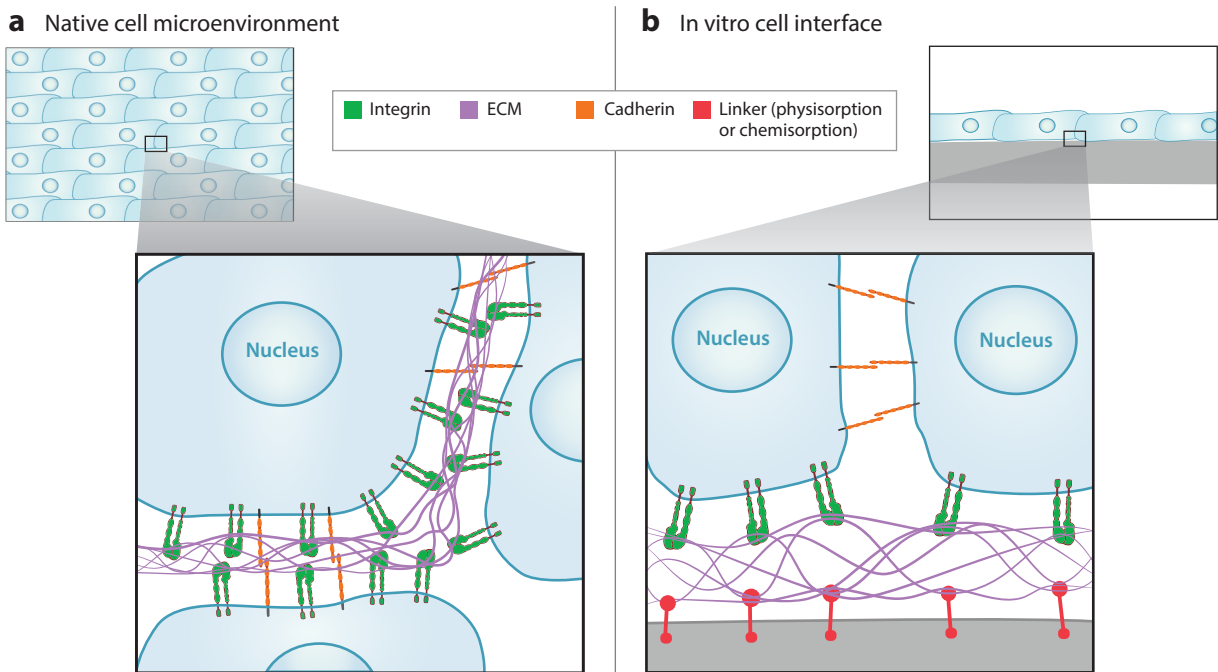


Figure 2

Simplified schematic highlighting interactions among integrins, extracellular matrix (ECM), cell–cell contacts, and linkers. (a) The native cell microenvironment can be mimicked by (b) the in vitro cell–substrate interface through the engagement of a cell’s integrins with specific ligands found within ECM proteins. The ECM in an in vitro interface is physically linked to the substrate (*gray*) via a linker (*red*). How a cell interacts (or not) depends on biochemical and biophysical properties of ECM, linker, and substrate. Note that the schematics are not drawn to scale.

Intercalated discs: provide mechanical and electrical coupling between CMs; also mediate intercellular signaling

Ligand: integrin binding site; different ligand types can be found in ECM proteins or peptide sequences

Substrate: material surface in direct contact with ECM protein or linker; depending on the type of biomaterial, the substrate could also be a biomaterial itself

embryonic versus adult tissues. During development, CMs display changing integrin expression profiles. The term integrin expression profile refers to the different integrin types and their respective quantities at the cell surface. Distinct integrin types can trigger different intracellular signaling pathways (24). Furthermore, during heart development the ECM exhibits changes in biochemical and biophysical properties such as biochemical composition as well as mechanical properties and structure. Changes in ECM properties ultimately lead to changes to the myocardium’s mechanical properties, which affect heart function. The CM integrin expression profile and surrounding myocardial ECM composition reach a dynamic steady state in adulthood, and upon disease or injury these properties undergo changes in expression and composition.

Embryonic and induced pluripotent stem cells (iPSCs) do not appear to have significant differences, and in this review we refer to both cell types as pluripotent stem cells (PSCs) (25, 26). PSC-derived CMs (PSC-CMs) are a model that allow the study of cardiac development, disease, and drug modeling. All in vitro setups require PSC-CMs to adhere to a substrate. However, cells do not directly interact with the substrate. A cell binds via integrins to specific binding sites on the ECM protein, which we refer to as the cell–ECM interface. The ECM protein is attached to the substrate via physisorption or a chemisorption linker (**Figure 2b**), which we refer to as the protein–substrate interface. We refer to the combination of the cell–ECM and protein–substrate interface as the cell–substrate interface (also known as the biointerface). How a cell interacts and responds to an in vitro microenvironment depends not only on the cell’s integrin type and ECM properties but also on the linker and substrate properties.

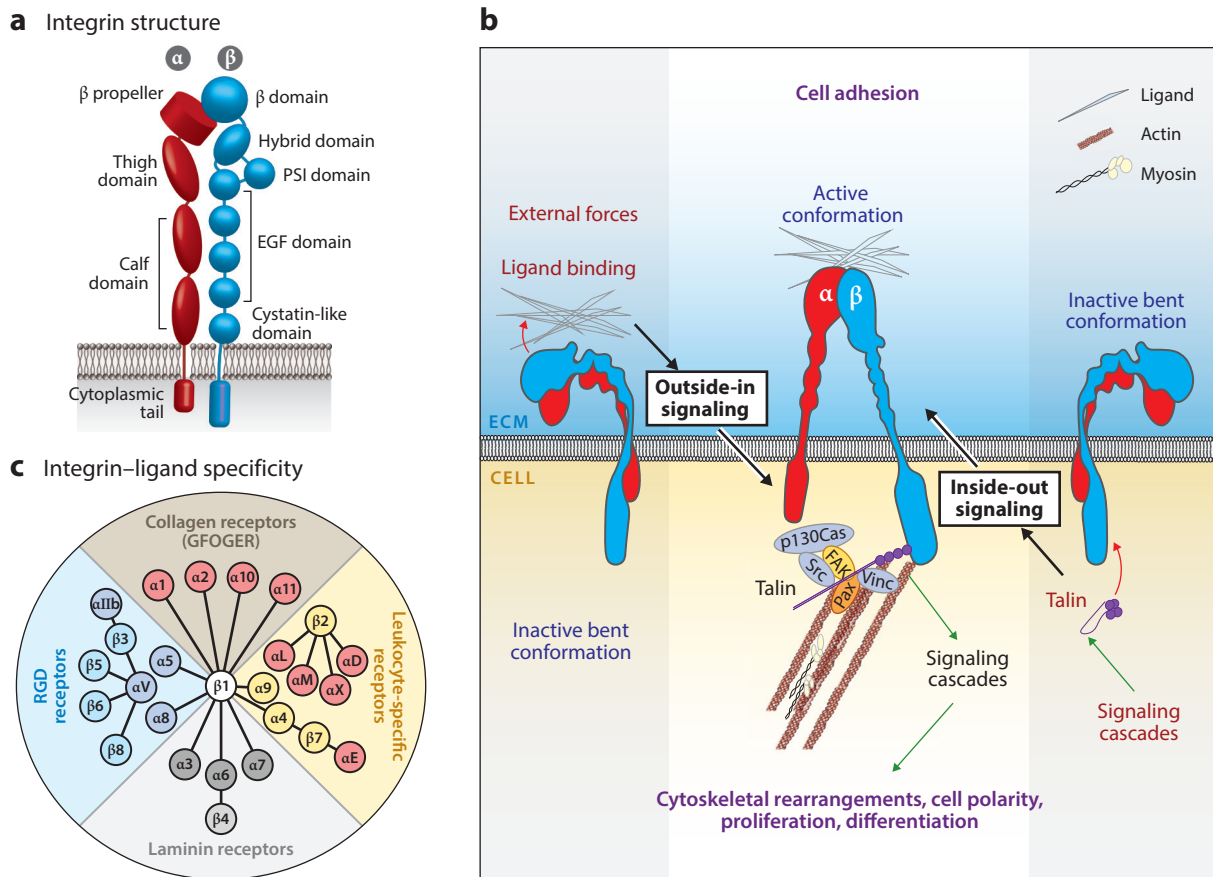


Figure 3

Integrins are cell adhesion receptors that serve as mechanical links between the extracellular matrix (ECM) and a cell's cytoskeleton. (a) Integrins are transmembrane heterodimers composed of an α and a β subunit. (b) Integrins are known as bidirectional signaling receptors that can trigger signaling cascades after externally binding to a ligand (outside-in signaling). Additionally, integrins can be controlled from signaling cascades within the cell (inside-out signaling). (c) Integrin subtypes have specific ECM protein ligand-binding properties. Panels adapted with permission from References (a) 155, (b) 156, and (c) 24, respectively.

One of the goals of *in vitro* platforms is to provide stem cells with the appropriate outside-in signaling needed for adhesion, cardiac lineage differentiation, and CM maturity by recapitulating aspects of the native cardiac microenvironment. PSC-CMs display early to late fetal CM characteristics in terms of morphology and function (27, 28). However, the lack of a suitable adult CM source and known differences between species (29) in terms of key cardiac contractile proteins (30) have motivated researchers to improve PSC-CM models and address the maturity challenge. Multiple *in vitro* approaches have been explored in an effort to increase PSC-CM maturity: electromagnetic stimulation, biochemical factors, physical stimulation (topography, stiffness, stretch), and long-term culture. The resulting models span from single cells to engineered tissues, such as engineered heart tissue, microfluidic heart-on-a-chip, cell sheets, decellularized heart, and muscular thin films (28, 31–34).

One way to probe and decouple the cell–substrate interface is by using biomaterials to vary different biophysical and biochemical properties (35). An open challenge for the field is to identify

Linker: connects ECM proteins to the substrate via physisorption (adsorption due to intermolecular forces) or chemisorption (adsorption involving a chemical reaction)

Cell–substrate

interface: in vitro region between cells and substrate that includes cell adhesion molecules (e.g., integrins), ECM proteins, linkers, and underlying material substrate; also known as the biointerface

Biomaterial: material designed to interact with cells; can be composed of ECM proteins or synthetic materials

Mechanobiology:

field dedicated to the study of the relationship between a cell and its physical environment

Immunohistochemistry (IHC):

method used to selectively label antigens (proteins) in tissue sections through specific antibody binding

the minimally complex biomaterial model that can support and recapitulate key features of cardiac function in cell and tissue models (36). Historically, Matrigel™ has prevailed for PSC culture and PSC-CM differentiation, though other synthetic alternatives are emerging. Matrigel's complex composition of more than 1,000 proteins and lot-to-lot variability complicate attempts to decouple the effects of ECM composition and contributes to heterogeneity in PSC-CM development and response. However, by systematically varying biomaterial properties, researchers are gaining better knowledge of the specific properties of CM differentiation, morphology, structure, function, and maturity.

To facilitate these efforts, we first review native developmental changes in CMs integrin expression and myocardial ECM composition. To support mechanobiological insights, we review strategies for linking ECM proteins to common substrates. Finally, we review a variety of biomaterials approaches that offer control over ligand composition, matrix mechanics (e.g., stiffness), dimensionality (e.g., two versus three dimensions), and matrix structure (e.g., topography) used in CM mechanobiology studies.

2. NATIVE CARDIAC DEVELOPMENT

2.1. Temporal Dynamics of Cardiomyocyte Integrin Expression (Development and Disease)

Integrins are heterodimers that consist of an α and a β subunit (**Figure 3a**). The size of individual subunits can range from 80 to 180 kDa. In mammals there are more than 18 α subunit and 8 β subunit types. To date, 24 unique α - β combinations (integrin types) have been identified. Spliced variant isoforms of individual subunits also exist (37). Different integrin types lead to specific integrin–ligand interactions. However, there is redundancy in the interactions, a specific integrin type can bind to different types of ligands, and one ligand can have multiple receptors for different integrin types (15). Specific integrin–ECM combinations (**Figure 3c**) have been extensively documented (24, 38). The result of ligand binding can be a broad range of signaling cascades within the cell (**Figure 3b**). Integrin function has been studied primarily via knockout animal models, and several functions remain unclear (24). For example, for fibroblast cells the $\alpha_5\beta_1$ integrin determines adhesion strength, while $\alpha_V\beta_3$ integrin and talin enable mechanotransduction (39). The integrin expression profile is also known to modulate the spatiotemporal organization of force transmission at cell–matrix adhesions (40). To bind an extracellular ligand, integrins at the plasma membrane must undergo a conformational change from bent to unfolded (**Figure 3b**). Biochemical and biomechanical integrin regulation affects integrin cell surface availability, binding properties, activation, and clustering (41).

The various methods used to determine integrin expression levels analyze either RNA levels or protein levels. Reverse transcriptase polymerase chain reaction (RT-PCR) provides a measure of the specific amount of target RNA. RNA sequencing provides the whole RNA transcriptome at one time point. A trade-off of these methods is that RNA data do not always translate directly to protein levels. Regulatory processes following the production of messenger RNA contribute to the mismatch between transcription and translation (42). While some studies use RNA levels to determine integrin expression, others favor the use of antibodies to directly label the protein. Western blot analysis quantifies relative protein expression levels. Immunohistochemistry (IHC) labeling of tissue sections with antibodies confirms protein expression and preserves the protein's spatial distribution. Fluorescence-activated cell sorting of labeled cells provides the relative protein levels from cell to cell. A caveat with antibodies is that care must be taken to validate and include appropriate controls to ensure the signal comes from the protein of interest and not nonspecific binding (43). A combination of both RNA and protein data would be the gold standard in integrin expression studies.

Table 1 Cardiomyocyte integrin expression in cardiac development and disease^a

Integrin subunit	Embryonic	Fetal	Neonatal	Adult	Disease/injury
α_1		■R (48)	■R (48)	×R (48)	↑R (48, 49)
α_3		■R (48)	■R (48)	■R (48)	→R (48, 49)
α_5	■M (45) α_5 is abundantly expressed	■R (48)	■R (48)	×M, R (15, 48)	↑R (48, 49)
α_6	■M (45, 46) α_6 is abundantly expressed	■M (46)	■M (46)		
α_7	■M (45)	■M (45)	■M (45)	■M (45) α_{7B} is abundantly expressed	↑M (51)
β_1		■R, M (45, 48)	■R (48)	■R, M, H (48, 52) β_{1D} is abundantly expressed	→R, A (48, 56) ↑M (55) ↓M (57, 58)

^aAll data are from cardiomyocyte protein expression. Myocardial tissue level trends are omitted. Filled squares indicate presence; crosses indicate absence. Upward arrows indicate an increase in expression; downward arrows indicate a decrease in expression; rightward arrows indicate no change in expression. Blank cells indicate no data. Abbreviations: A, rabbit; H, human; M, mouse; R, rat.

In this section, we review CM integrin expression throughout normal cardiac development and describe how it changes with different cardiovascular diseases. Integrins are at the cell–ECM interface and thus are essential to mechanobiological signaling during these remodeling phases (44). The studies reviewed use various animal models, and we note that differences may exist between species, including in integrin expression. Thus, we provide the model organism in parentheses for clarity.

In early cardiac muscle development, CMs express α_5 and α_6 integrin subunits dimerized with both β_{1A} and β_{1D} (mouse) (45). The α_5 integrin subunit is replaced by α_7 in adult CMs (mouse) (46). CM integrin subunit expression undergoes a switch at birth, and $\alpha_{7B}\beta_{1D}$ integrin becomes dominantly expressed (mouse) (45). **Table 1** summarizes trends in CM integrin expression throughout development and with disease/injury. The α integrin subunits expressed in CMs also include α_1 , α_6 , α_9 , and α_{10} (9). In addition to the dominant β_1 integrin subunit, β_3 and β_5 are present in CMs (9).

2.1.1. α_1 . $\alpha_1\beta_1$ integrin is associated with cell attachment to collagen and laminin (47). The α_1 integrin subunit is present in fetal and neonatal CMs (rat) (48). However, by the time CMs reach adulthood, the α_1 integrin subunit is no longer present (rat) (48). Induction of cardiac hypertrophy by aortic coarctation revealed increased expression of the α_1 integrin subunit in CMs (rat) (48). In an induced myocardial infarction (MI) model, the α_1 integrin subunit localized to CMs in the peri-infarcted area and increased from undetectable to detectable levels 1 week post MI and persisted until 6 weeks post MI (rat). Expression of α_1 integrin also increased in apoptotic CMs after MI (49).

2.1.2. α_3 . $\alpha_3\beta_1$ integrin is known to bind to laminin (47). Terracio et al. (48) showed that the α_3 integrin subunit is present in fetal, neonatal, and adult CMs (rat). They induced cardiac hypertrophy by aortic coarctation and observed no change in α_3 integrin subunit expression levels in CMs (rat) (48). Nawata et al. (49) induced MI and observed no change in the level of expression of the α_3 integrin subunit in CMs throughout the 6 weeks after MI (rat).

2.1.3. α_5 . $\alpha_5\beta_1$ integrin is known to bind to fibronectin (47). Embryonic CMs express the α_5 integrin subunit, which is found in complex with both β_{1A} and β_{1D} (mouse) (45). Wiencierz et al. (46) confirmed that in embryonic CMs the α_5 integrin subunit is strongly expressed (mouse). The α_5 integrin subunit is present in fetal and neonatal CMs (rat) (48). However, by the time CMs reach adulthood, the α_5 integrin subunit is no longer present (rat, mouse) (15, 48). Terracio et al. (48) induced cardiac hypertrophy and observed the return of the α_5 integrin subunit in CMs (rat). Nawata et al. (49) induced MI and observed a peak in the level of expression of the α_5 integrin subunit in CMs at 4 and 7 days post MI (rat). The level of expression then decreased to levels observed in control groups after 6 weeks post MI (rat). The disparity in temporal dynamics of α_5 and α_1 integrin subunit expression following MI suggests that different α integrin subunits could have different roles in remodeling (44, 49).

2.1.4. α_6 . $\alpha_6\beta_1$ integrin is known to bind to laminin (47, 50). Embryonic CMs express the α_{6A} integrin subunit, which is found in complex with both β_{1A} and β_{1D} subunits (mouse) (45). Wiencierz et al. (46) confirmed that in embryonic CMs, α_6 is a strongly expressed integrin subunit (mouse). At the tissue level, early in embryonic development, the α_6 integrin subunit is located primarily in the heart and specifically within the myocardium (mouse), and it is no longer present in the myocardium by birth. Expression of the α_6 integrin subunit is spatially regulated as the heart matures; it is initially downregulated in the ventricles, followed by the atrial regions. The α_6 integrin subunit is also present in early chick myocardium (15). Recently, atrial and ventricular CM subpopulations were isolated throughout embryonic and adult stages based on differential expression in the α_6 integrin subunit (mouse). Patch-clamp analysis and gene expression profiling confirmed the atrial and ventricular CM subtypes. Expression levels of the α_6 integrin subunit correlated with expression of myosin light chain 2a (MLC-2a) and MLC-2v (46).

2.1.5. α_7 . $\alpha_7\beta_1$ integrin is known to bind to laminin (47). Braccaccio et al. (45) found that the α_{7B} integrin subunit in CMs starts to be expressed at embryonic day (E)17 (mouse). $\alpha_{7B}\beta_{1D}$ integrin is present in developing and adult CMs (mouse) (45). The onset of α_7 integrin subunit expression in CMs during cardiac muscle development is not temporally coordinated with β_{1D} expression (mouse) (45). Following birth and in adulthood, the α_7 and β_{1D} integrin subunits are abundantly expressed in CMs (mouse) (45). Babbitt et al. (51) demonstrated that the α_7 and β_{1D} integrin subunits in CMs increase in expression 1 week following aortic constriction (mouse).

2.1.6. β_1 . The β_1 integrin subunit is ubiquitous in many cell types and is present in half of known integrin types (24). The β_1 integrin subunit is present in fetal, neonatal, and adult CMs (rat) (48). The initial expression time point of the β_{1D} integrin subunit varies between studies within the same species. Braccaccio et al. (45) showed that from E11 to E17 the β_{1A} and β_{1D} integrin subunit variants are coexpressed in CMs (mouse). In contrast, Van Der Flier et al. (52) showed that β_{1D} integrin subunit expression in CMs begins around the time of birth (mouse). In the developing and newborn heart, β_{1D} can dimerize with several α integrin subunits, including α_5 , α_7 , and α_{7B} (mouse) (45). This study showed that β_{1D} is not an exclusive partner to α_{7B} , as was previously thought. As development progresses, β_{1A} subunit expression progressively declines, while β_{1D} subunit expression increases in CMs (mouse) (45). In newborn and adult CMs, the integrin subunit isoform β_{1D} is the only β_1 subunit expressed (mouse) (45). Van Der Flier et al. (52) also showed that the β_{1D} integrin subunit was present at the costameres and intercalated discs of adult CMs (mouse and human). The integrin subunit β_{1D} may provide muscle cells with a stronger mechanical link between the ECM and actin cytoskeleton fibrils (53). Moreover, in adult CMs, the β_{1D} integrin subunit associates only with the α_{7B} integrin subunit (mouse) (45).

Terracio et al. (48) induced cardiac hypertrophy and observed no change in β_1 integrin subunit expression levels in CMs (rat). Sun et al. (54) demonstrated that gene expression of β_1 is temporally upregulated after MI (rat). Additionally, these authors showed that β_{1D} is downregulated by inflammatory cytokines such as tumor necrosis factor. Krishnamurthy et al. (55) observed an increase in β_1 integrin subunit expression in CMs after MI in comparison to controls (mouse). They also noted that not all CMs exhibit increased β_1 expression. Ichikawa et al. (56) demonstrated that after 9 weeks of treatment with daunorubicin (a cardiotoxic drug reducing left ventricular function) the total protein expression of β_{1D} did not change in comparison to controls (rabbit). Manso et al. (57) showed that loss of talin-2 led to a 50% reduction in levels of β_{1D} in CMs, while normal cardiac structure and function were maintained (mouse). Transgenic mice overexpressing thrombospondin 3 (Thbs3; upregulated in cardiac disease) in CMs showed reduced surface integrin and sarcolemma stability. β_{1D} , α_5 , and α_7 integrins from Thbs3 hearts showed reduced membrane presence (mouse). Overexpression of $\alpha_7\beta_{1D}$ integrin reduced Thbs3-related disease and led to a rise in endogenous integrin $\alpha_5\beta_{1D}$ (mouse) (58).

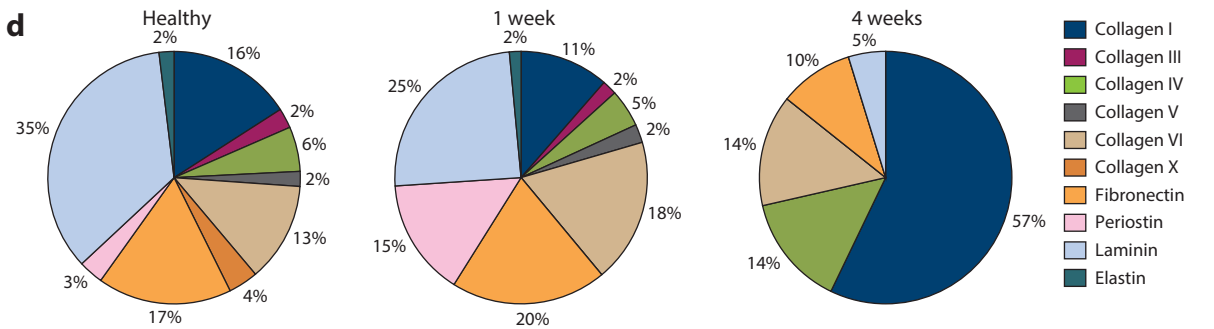
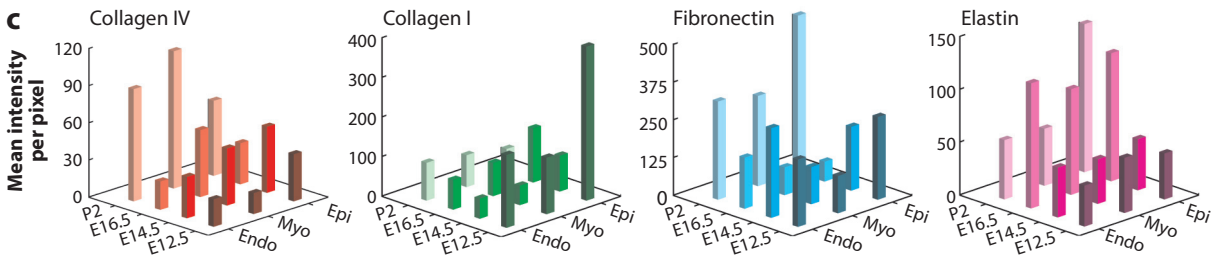
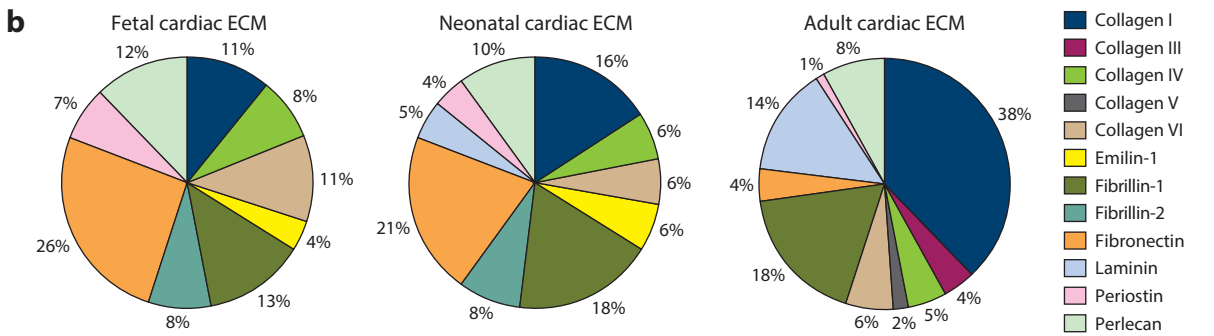
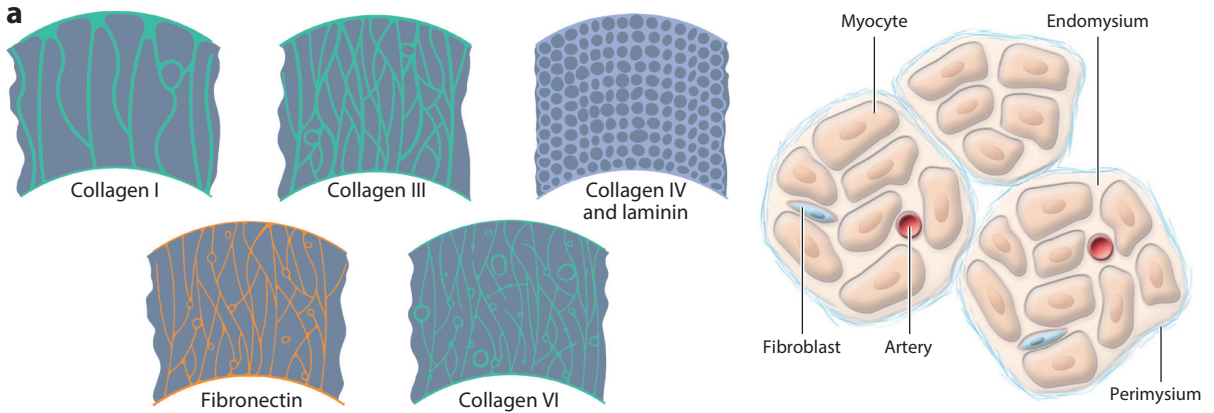
2.1.7. Pluripotent stem cell and pluripotent stem cell–cardiomyocyte integrins. Much less is known about the integrin expression of PSC-CMs. PSCs abundantly express α_5 , α_6 , α_V , β_1 , and β_5 integrin subunits (59). The PSC-CM integrin expression profile has been shown to be temporally modulated. Ja et al. (60) demonstrated that PSC-CMs express higher RNA levels of α_1 , α_2 , α_3 , α_7 , and β_1 integrin subunits than do PSC cardiac progenitors (human). Yu et al. (61) showed that α_7 integrin subunit expression is lower in PSC-CMs than in neonatal CMs (mouse).

2.2. Temporal Dynamics of Myocardial Extracellular Matrix Composition (Development and Disease)

In order to evaluate the native cardiac ECM proteome, samples must be in the form of whole tissue sections or isolated/enriched ECM proteins from tissues. IHC has been used to spatially label ECM proteins within tissue sections. As discussed above, trade-offs concerning the use of antibodies apply. A few studies have also reported ECM gene expression levels using RT-PCR. Another common technique involves decellularization of the heart and a protein precipitation step, followed by analysis via liquid chromatography in tandem with mass spectrometry (LC-MS/MS) (62). A drawback of performing decellularization is that some soluble matrix components can be lost or altered during sample processing (63). Missing low-abundance proteins are a known pitfall of LC-MS/MS (62). Ongoing challenges in cardiac proteome analysis include the relative insolubility of ECM proteins and the relatively high abundance of other proteins in cardiac tissues (64).

In this section, we review the changes that occur in myocardial ECM composition throughout the normal cardiac development timeline. We also discuss ECM protein structural organization and spatial location within the myocardium (**Figure 4a**). We then describe how the myocardial ECM composition profile is affected by different cardiovascular diseases. Unless otherwise stated, the following discussion describes composition changes within the left ventricle. There exist many differences among species, and while some myocardial ECM composition changes may be the same, we list the model organism in parentheses for clarity. **Table 2** summarizes trends in myocardial ECM protein composition in cardiac development and disease. For coverage of other cardiac ECM proteins and composition of other heart compartments, we refer the reader to other excellent detailed reviews (2, 65).

2.2.1. Collagens. Collagen fibrils are aggregates of triple helices composed of long polypeptide chains called α chains (66). Individual collagen fibrils, with diameters ranging from 30 to



(Caption appears on following page)

Figure 4 (Figure appears on preceding page)

(a) The myocardial ECM is composed of a hierarchical network of proteins with distinct dominant spatial distributions. (b) The ECM protein composition dynamically changes throughout cardiac development (fetal, neonatal, adult stages). (c) ECM compositional changes vary among distinct heart tissue layers (Endo, Myo, Epi) during developmental stages (12.5, 14.5, 16.5, and P2). (d) In addition, ECM protein composition dynamically changes after myocardial infarction. Abbreviations: ECM, extracellular matrix; Endo, endocardium; Epi, epicardium; Myo, myocardium; P2, postnatal day 2. The numbers 12.5, 14.5, and 16.5 refer to embryonic days 12.5, 14.5, and 16.5, respectively. Panels adapted with permission from References (a) 63 and 157, (b) 74, (c) 70, and (d) 76.

80 nm, come together to form collagen fibers (66). The 14 different types of collagen vary in their composition and arrangement of α chains (66). Collagens I, II, III, V, and XI form fibrils, and the rest are described as nonfibrillar (66). Collagen is the most abundant ECM protein in the heart. The myocardial collagen matrix is 75–80% collagen I; 11–20% collagen III; and the remaining percentage composed of collagen IV, collagen V, and collagen VI (63, 66). This ratio of collagen types has also been reported to be conserved among three species (rat, dog, and macaque) (67).

The adult myocardium has a collagen network with a hierarchical structure that evolves during development. Within the endomysium (**Figure 4a**), neighboring CMs are connected by intercellular struts composed of collagen fibrils and anchored near the Z-band level (66). CMs are next surrounded by interwoven bundles of collagen fibrils, and the perimysium (**Figure 4a**), which contains collagen bundles that surround groups of CMs (66).

Endomysium: fine connective tissue septum that surrounds each individual CM

Perimysium: large connective tissue septum that surrounds groups of CMs

Table 2 Myocardial ECM protein composition in cardiac development and disease^a

ECM protein	Embryonic	Fetal	Neonatal	Adult	Disease/injury
Collagen I	■M (70)	■R (72–74)	↓M (70) ↑R (72–74)	↑R (72–74) Collagen I is abundantly expressed	↑R (75, 77) ↓R (76)
Collagen III		■R (73, 74)	↑R (74)	↑R (73, 74)	↑R (75) →R (77) ×R (76)
Collagen IV	■M (70)	■R (73, 74)	↑M (70) ■R (73) ↓R (74)	■R (73) ↓R, (74) Collagen IV is a major component of basement membrane	↑R (76, 77)
Collagen V			■R (72)	■R (76)	↓R (76)
Collagen VI				■R (67)	↑R (76)
Collagen XV				■R (76)	×R (76)
Laminin	■H (83)	■R (73)	↑R (73)	↑R (73) ■H (84) Laminin is a major component of basement membrane	↓R (76) →R (77)
Fibronectin	■M (70)	■R (74) Fibronectin is abundantly expressed	↓R (74) →M (70) Fibronectin is abundantly expressed	↓R (74)	↑H, R, M (49, 76, 85, 87, 88)
Elastin	■M (70)		→M (70)	■R (77)	→R (76, 77)

^aAll data are from myocardial left ventricular ECM protein expression. Trends in the disease column reflect the first temporal data point reported. Filled squares indicate presence; crosses indicate absence. Upward arrows indicate an increase in expression; downward arrows indicate a decrease in expression; rightward arrows indicate no change in expression. Blank cells indicate no data. Abbreviations: ECM, extracellular matrix; H, human; M, mouse; R, rat.

A changing composition of collagens contributes to the complex mechanical properties and function of the myocardium (66, 68). Important factors include spatial location and relative alignment, fiber structure and dimension, fiber density, and fiber cross-linking (66, 68). For example, collagen composition changes dramatically with fibrosis, a compensatory remodeling mechanism that involves changes in the ECM that preserve the tissue's integrity. Many cardiac diseases increase the deposition or rearrange the organization of collagen, and imaging methods sensitive to collagen I and collagen III have been applied to observe this progression (63). In general, with age, the myocardium's collagen concentration and number of cross-links increase (66). This increase in collagen within the myocardium increases muscle stiffness (66).

2.2.1.1. Collagen I. Collagen I is secreted from fibroblasts as procollagen, self-assembles into fibrils after being modified by enzymes, and is stabilized by covalent cross-links across the triple-helix structure (63, 66). Collagen I fibers are typically composed of thick, densely packed fibrils with an average diameter of 75 nm (66). At the adult stage, collagen I is located at high abundance in the perimysium and at lower abundance in the endomysium (rat) (**Figure 4a**) (67, 69). A key role of collagen I is to provide structural support and strength within the myocardium (67, 70). Collagen I is a relatively stiff material that exhibits high tensile strength and provides rigidity (66, 71).

When observed for a period extending up to postnatal stage (P)2 (mouse), collagen I expression in the myocardium is highest at E12.5 (**Figure 4c**) (70). The lower amount of collagen I in the myocardium during initial stages of development is thought to contribute to tissue elasticity during expansion (70). In contrast, the same study showed that collagen I gene expression increased from E12.5 to P2 (70). Studies using rat myocardium observed collagen I increasing steadily throughout the fetal, neonatal, and adult stages (**Figure 4b**) (72–74). As the heart's functional capacity develops to meet the higher workload from E12.5 to P2, the collagen network within the ventricles increases in spatial mesh complexity and fiber structure (70). After birth, the speed at which the collagen network develops increases drastically, reaching adult structure within 20 days postpartum (rat) (72). The amount of collagen I does not change within 20 days postpartum (72). The adult heart has a significantly higher amount of collagen I versus the fetal heart (73). Collagen I is the most abundant protein in the adult heart (rat) (74).

Aging and several diseases or injuries can cause changes in expression of collagen I. As the myocardium ages, collagen I concentration increases substantially, and the number of fibers and thickness increase as well (63, 66). Collagen I is crucial for heart tissue repair after injury or disease. If loss of CMs occurs, cardiac fibroblasts are recruited to the damaged region and compensate for muscle loss primarily by secreting collagen I (63). One study found that collagen I increased at 4 weeks post MI and remained elevated at 10 weeks (rat) (75). In the same study, collagen I within the right ventricle peaked at 4 weeks post MI and started to decline toward baseline at 10 weeks (75). This study highlights the temporal dynamics of the ECM as a function of spatial localization within the heart. One week after MI there was a small decrease in collagen I, but by week 4 the amount of collagen I had increased above healthy baseline values (rat) (**Figure 4d**) (76).

2.2.1.2. Collagen III. Collagen III is a homotrimer that forms a compliant fiber network (63). Collagen III fibers are typically composed of thin, loosely packed fibrils with an average diameter of 45 nm (66). Collagen III is secreted by smooth muscle cells and fibroblasts (66).

At the adult stage, collagen III is more abundant in the endomysium and less so in the perimysium (**Figure 4a**) (67). Collagen III exhibits high tensile strength, contributes to structural support, and provides elasticity (66, 71). A metric of relative stiffness within cardiovascular tissue is the ratio of collagen I to collagen III. This ratio is high during the human neonatal stage and

contributes to a rigid heart during early development, then decreases after birth and reaches a steady state in adulthood (71). A crucial function of collagen III is regulation of collagen I fibrillogenesis, making it necessary for normal cardiovascular development (63, 73).

Collagen III significantly increases as the heart matures from the fetal to adult stage (rat) (73). A rat study showed an increase in collagen III concentration from the fetal to the neonatal to the adult stage (**Figure 4b**) (74). Collagen III transiently increased at 2 weeks post MI, then declined to baseline values at 4 weeks (rat) (75). In another recent MI study, collagen III did not significantly change expression over the 8-week observation time (rat) (77). The variations in temporal expression in these two studies could be due to differences in sample preparation and analysis (77). In another adult rat MI study, collagen III was no longer present 4 weeks post MI (**Figure 4d**) (76).

2.2.1.3. Collagen IV. Collagen IV is nonfibrillar, with three heterotrimer variants composed of six different α chains (63). Both cardiac fibroblasts and CMs secrete collagen IV (20). In adult myocardium, collagen IV is confined to the basement membrane of myocardial, endothelial, and smooth muscle cells (**Figure 4a**) (67). The basement membrane is rich in collagen IV (78). Furthermore, collagen IV is present along the T-tubular network and is thought to provide structural support during contraction (65, 69). Collagen IV serves as a cell-adhesive protein and links groups of CMs to the surrounding ECM (66).

Collagen IV increases in density and organization from E12.5 to P2 (mouse) (**Figure 4c**) (70). At E14.5, collagen IV surrounds CMs in a disconnected circular configuration. By the postnatal stage, the collagen IV network was more interconnected throughout the myocardium and has a more fibrillar structure (70). Within 3 days of birth, the collagen IV network becomes denser in the endomysium (72). Collagen IV does not undergo any significant changes in expression during the fetal, neonatal, or adult phase (rat) (73). Conversely, another study showed that collagen IV decreases during fetal, neonatal, and adult phases (rat) (**Figure 4b**) (74). After MI, the amount of collagen IV increased, reached a maximum at 2 weeks post MI, and then progressively decreased (rat) (77). In another adult rat MI study, at week 4 the amount of collagen IV remained above healthy baseline values (**Figure 4d**) (76).

2.2.1.4. Other collagen types. Other collagens found in cardiac tissue include collagen V, collagen VI, and collagen XV. In a postnatal rat model, collagen V is located in the endomysium and basal lamina (a component of the basement membrane) (72). In an adult rat MI study, collagen V was no longer present 4 weeks post MI (76). In adult rat myocardium, collagen VI is abundant in the endomysium and less in the perimysium (**Figure 4a**) (67). In an adult rat MI study, 1 week post MI there was a small increase in collagen VI, and by week 4 the level approached healthy baseline values (**Figure 4d**) (76). Furthermore, a knockout study found that a collagen VI-deficient mouse had a reduction in chronic CM apoptosis and fibrosis compared with wild-type mice, which led to improved cardiac function after MI (79). Collagen XV is involved with ECM organization within the heart (80). In an adult rat MI study, collagen XV was no longer present 4 weeks post MI (76).

2.2.2. Laminin. Laminins are a family of glycoproteins that form a T-shaped heterotrimer and are composed of one α , one β , and one γ chain (63). Fibroblasts and CMs can secrete laminin (20). Laminin is found in the basement membrane of cardiac tissue and vasculature (67). Laminin forms a fine network and is a major component of the basement membrane (**Figure 4a**) (78, 81). The basement membrane in adult rat cardiac ventricles has a striated laminin structure with a length similar to that of sarcomeres (78). Laminin is the first ECM protein observed in the developing embryo and has an essential role in anchoring cells to ECM (81). Another function of laminin is to cross-link other ECM proteins, including collagen IV, perlecan, and entactin (82).

Tissues from humans at gestational week 8 showed that the laminin β_1 and laminin β_2 chains are present in the ECM surrounding CMs (83). In a rat model, the amount of laminin significantly increased during the fetal, neonatal, and adult phases (73). Another rat study confirmed the increase in laminin from the fetal to the neonatal to the adult stage (**Figure 4b**) (74). Transcriptome expression data of adult myocardium indicate abundant expression of laminin-221, and protein studies confirmed its presence (human) (84). In an adult rat MI study, 1 week after MI there was a decrease in laminin, which was further reduced by the fourth week (**Figure 4d**) (76). In another recent rat MI study, the amount of laminin did not significantly change over the 8-week observation period (77).

2.2.3. Fibronectin. Fibronectin is a glycoprotein with a rodlike structure that is composed of two subunits connected by disulfide bonds (63). The subunits consist of repeating modules (types I, II, and III). At the adult stage, fibronectin is more abundant in the endomysium and less so in the perimysium (**Figure 4a**) (67). It is generally thought that fibronectin has a role in connecting the surface of CMs to the endomysium (72). Fibronectin plays an essential role during cardiac development via adhesion, migration, and differentiation, and it also plays a beneficial role during the wound healing process (63, 85, 86). Combinations of different subunits allow fibronectin to have different cell-binding properties and to cross-link with other ECM components (70). Fibronectin has a strong affinity for collagen III and also binds to collagen I, fibrin, heparin, and syndecan (70, 72).

In rat myocardium, fibronectin was the most abundant protein in the fetal and neonatal stages (**Figure 4b**) (74). The amount of fibronectin decreases significantly from fetal to adult age (**Figure 4b**) (63, 73, 74). The organization of fibronectin increases during early stages of development. In mouse myocardium, at E14.5 fibronectin formed thin, isolated fibrils, and by P2 the network had become more interconnected (70). Throughout the observation window of these early time periods (E14.5–P2), the amount of fibronectin remained relatively constant (**Figure 4c**) (70). A study in a human heart after MI showed that fibronectin deposition rapidly increased within and around the infarcted area from 12 h to 14 days post MI (87). Accumulation of fibronectin was also observed in a rat model 4–35 days post MI (85). Results from another adult rat MI study showed a small increase in fibronectin 1 week post MI (76). By 4 weeks post MI, the amount of fibronectin was below control values (**Figure 4d**) (76). Following similar trends, a rat MI study showed fibronectin increasing in the peri-infarcted area 1 week post MI, and 6 weeks post MI expression decreased (49). In a mouse pressure overload study, fibronectin accumulation increased over 4 weeks (88).

2.2.4. Elastin. Elastin is composed of tropoelastin monomers that contain alternating hydrophobic and hydrophilic domains (63). Within the myocardium, elastin is located within the interstitium and in the walls of coronary blood vessels (68). A major structural function of elastin is to provide elasticity to the myocardium during cyclic loading (70). Furthermore, elastin is essential to heart development and vasculature.

In the developing mouse myocardium (E12.5–P2), levels of elastin remained constant, with a transient peak at E16.5 (**Figure 4c**) (70). At P2, elastin in the myocardium was organized into fibrils (70). The transient elastin peak is thought to provide the elasticity needed to accommodate the increased growth and workload (70). It is also thought that the relative decrease in elastin after birth may contribute to the maturation of CMs and their sarcomeres (70). In a rat study, the elastin concentration did not significantly change throughout the 8 weeks after MI (77). In another adult rat MI study, the elastin amount was unaltered 1 week post MI, and by 4 weeks post MI, elastin was no longer detected (**Figure 4d**) (76). Post-MI mouse models indicate that fibrotic tissue is

composed mostly of collagen I but also elastin, with tropoelastin significantly increased between 7 and 21 days post MI (89). The role of elastin during fibrosis is to preserve elasticity.

3. IN VITRO PROTEIN–SUBSTRATE INTERFACE

In vitro CM mechanobiology studies allow researchers to probe a cell's intrinsic properties and quantitatively measure its response. One way in which the in vitro cell–substrate interface differs from the native cell microenvironment is that the ECM protein is attached to the substrate via a linker (**Figure 2a,b**). Two common substrates in mechanobiology studies are polyacrylamide (PA) hydrogels and polydimethylsiloxane (PDMS) (90, 91). We review various linking strategies used to attach ECM proteins to the substrate and discuss differences in binding strength to the substrate.

3.1. Polyacrylamide Hydrogels

PA hydrogels are made up of a network of cross-linked acrylamide monomers. PA hydrogel properties, including stiffness and porosity, are determined by monomer and cross-linker concentration (92). These variables can be tuned to create PA hydrogels with a wide range of physiologically relevant stiffnesses, useful for mechanobiology studies. Here we review methods used to attach proteins to PA hydrogel surfaces.

3.1.1. Covalent chemistries to bind proteins to polyacrylamide hydrogels. Attaching ECM proteins to the surface of a PA hydrogel for mechanobiology studies is nontrivial. The ECM protein is commonly attached to a substrate via physisorption or a chemisorption linker. PA hydrogels have no ability to adsorb protein (93). PA hydrogel copolymerization with ECM proteins enables the proteins to be present at the surface or distributed throughout the network (94, 95). Copolymerization is beneficial because it bypasses the need for surface modifications to attach proteins. However, the exact linking mechanism of copolymerization is not known. PA hydrogels must be modified in order to use a chemisorption linker to attach proteins.

Many protein adhesion methods create covalent bonds between the protein and the substrate via side chains that are introduced to the surface of the PA hydrogel. Covalent attachments are the most secure way to bind proteins to PA hydrogels (96). Sulfosuccinimidyl 6-(4'-azido-2'-nitrophenylamino)hexanoate (sulfo-SANPAH) is frequently used as a covalent linker between proteins and PA hydrogels (97–99). Sulfo-SANPAH is a heterobifunctional cross-linker with a phenylazide and a *N*-hydroxysuccinimide (NHS) ester group. When activated by light, the phenylazide group binds to any chemically stable molecule (including the PA substrate) via a nonspecific covalent bond. The NHS ester group on the other end of the cross-linker binds to the amines in the protein (100). Another surface modification method used to bind proteins to PA hydrogels involves hydrazine hydrate. Hydrazine hydrate is a reducing agent that converts inert amide groups on the surface of the PA hydrogel into hydrazine groups, which readily react to form covalent bonds with the aldehyde or ketone groups in proteins (92).

Linkers can also be added to the PA precursor solutions and dispersed throughout the hydrogel. Many of them work in a similar manner as sulfo-SANPAH, in that a linker forms a bond to amines in the protein's backbone. Examples include NHS acrylate (101), 6-acrylaminoethylaminohexanoic acid *N*-succinimidyl ester (N6) (102), and 1-ethyl-3-(3-dimethylaminopropyl)carbodiimide (EDC) (95). NHS acrylate and N6 add ester groups that bind to amines in the protein's backbone (102), while EDC is used to add carboxylic groups that bind to a protein's amine backbone (95).

While side-chain chemistries have been widely used, researchers have concerns about the variability and lack of control of protein specificity. Due to the nonspecificity of the bond, protein presentation is highly variable in terms of both the number and location of binding sites (90, 99). These concerns have led to the development of site-specific protein immobilization techniques. One molecule, 2-pyridinecarboxaldehyde, immobilizes proteins on their N termini and can successfully immobilize collagen, fibronectin, and laminin (90, 103).

3.2. Polydimethylsiloxane

PDMS is a silicone-based polymer made by mixing prepolymer with a cross-linker. PDMS is low cost, transparent, and readily molded into various geometries and setups, making it a versatile substrate for mechanobiology studies. Due to its hydrophobic nature, PDMS does not bind specifically to proteins well (104). Here we discuss different methods used to attach proteins to PDMS substrates.

3.2.1. Adsorption of proteins onto polydimethylsiloxane. Physisorption is a common means of attaching proteins to PDMS substrates (91, 105–112). Plasma surface treatment of the PDMS is used to encourage protein adsorption. Oxygen plasma inundates the PDMS surface, resulting in silanol groups that make the surface hydrophilic and increase protein adsorption (110, 111, 113). PDMS surface roughness does not change upon plasma treatment; however, after protein adsorption the surface becomes rough (112). Plasma treatment alone can be used to adhere specific cell types directly to PDMS. Cells adhere selectively to plasma oxidation–patterned regions (114). The protein–substrate interactions caused by adsorption are weak van der Waals bonds (115). The bond strength of adsorbed proteins on PDMS is around 1 kN/m², and cells exerting a higher traction force can break this bond and detach (116).

3.2.2. Covalent chemistries to bind proteins to polydimethylsiloxane. Methods of bonding proteins to PDMS surfaces rely on adding reactive groups to the surface (104, 117, 118), which allows for the formation of covalent bonds between the protein and substrate. A common strategy employed with PDMS uses two molecules; the first molecule adds amine groups to the PDMS surface, and the second molecule links the added amine groups to the protein. A combination of (3-aminopropyl) triethoxysilane (APTES), which adds amine groups to the PDMS substrate, and glutaraldehyde (GA), which links the amine groups to the protein, is frequently used in such strategies (104, 117). This specific combination has been utilized to bind various proteins, including collagen (117), Protein A (106), and fibronectin (117). Other molecules that can be used in place of GA include ascorbic acid (118) and EDC (104). Distinct chemisorption linkers lead to differences in attached protein density. The protein attachment methods can be ranked from highest to lowest protein density as follows: APTES/EDC, APTES/GA, GA, and physisorption (104).

Another protein attachment method involves adding reactive groups throughout the PDMS prepolymer mixture. Phospholipids conjugated to functional groups can serve as chemisorption linkers. Some phospholipids will be exposed on the PDMS surface and can present functional groups to bind proteins (119).

Sulfo-SANPAH is commonly used to functionalize proteins on PDMS substrates. However, it does not covalently bind proteins to PDMS, as discussed in the following section (99).

3.3. Bond Strength of the Linker at the Protein–Substrate Interface

In both PA hydrogel and PDMS substrates, chemistries are used to covalently bind proteins to the substrate. Protein attachment is essential for stable and consistent culture of cells on the

substrate. Adhesion between protein and substrate can regulate cell behavior (116). A mechanical test machine measured the protein–substrate binding strengths to be 1.28 kN/m² and 11.9 kN/m² for proteins adsorbed and covalently bound to PDMS, respectively. Focal adhesion size and actin cytoskeleton organization were higher in covalently versus adsorption-bound substrates (116).

Characterization of the protein–substrate interface and binding strength of the linker to the substrate can be used to compare cellular responses among different substrates and linkers. Protein–substrate adhesion strength can be varied with different linker strategies. As discussed above, the linker sulfo-SANPAH forms covalent bonds with the PA hydrogel network. Characterization via atomic force microscopy demonstrated that proteins cannot be covalently bound to PDMS via sulfo-SANPAH, because PDMS does not contain free amines (99). This study also showed that ultraviolet treatment of PDMS in the presence of sulfo-SANPAH does not add amine groups to the surface or change the strength of the bond between PDMS and protein (**Figure 5a**). Instead, PDMS can be treated with APTES, resulting in the addition of primary amines on the surface that then react with the sulfo-succinimidyl group of sulfo-NHS-biotin to form a covalent bond (**Figure 5c**). PA hydrogel/sulfo-SANPAH/collagen has a binding strength comparable to that of PDMS/APTES+sulfo-NHS-biotin (**Figure 5b**).

4. IN VITRO BIOMATERIALS APPROACHES TO RECAPITULATE THE CARDIOMYOCYTE MICROENVIRONMENT

The microenvironment's biochemical and biophysical properties modulate CM adhesion, morphology, differentiation, cytoskeleton structure, mechanical output, contractility, and degree of maturity. Biomaterials can be leveraged to systematically tune the properties of a cell's microenvironment (35). The complexity of cell-adhesive domains, reproducibility, and tunability is a function of biomaterial sources (naturally derived, hybrid/semisynthetic, fully defined) (120). Decellularized cardiac tissue incorporates the complexity of native myocardium's ECM composition and structure but offers limited ability to modulate the cell–substrate interface (120–123). For a more in-depth discussion of biomaterial approaches designed to support CM differentiation and maturity, we direct the reader to several excellent reviews (124–126). In the following subsections, we review biomaterial approaches to the control of ligand composition, matrix mechanics (e.g., stiffness), dimensionality (e.g., two versus three dimensions), and matrix structure (e.g., topography) used in CM mechanobiology studies.

4.1. Ligand Composition

Ligand composition influences both cell adhesion and differentiation toward specific lineages. The native myocardial ECM composition changes throughout cardiac development. ECM ligand composition in vitro can be varied by using individual or a combination of ECM protein types. Ligand composition can influence CM adhesion. Borg et al. (127) observed that adult rat CMs adhere more efficiently to laminin and collagen IV than to other proteins, while neonatal CM adhesion does not depend on protein type. Changes in integrins and other ECM receptors are likely responsible for these observed differences in cell adhesion (63). Burrige et al. (128) compared multiple defined proteins, including recombinant human E-cadherin, recombinant human vitronectin, recombinant human laminin-521, truncated recombinant human laminin-511, and vitronectin peptide. All of them supported efficient PSC cardiac differentiation; however, the laminin-based proteins best supported long-term (day 15+) adhesion of PSC-CMs. Differences in integrin–ECM protein interactions are thought to be responsible for the observed CM adhesion. Human recombinant laminin-211 also supports small-molecule-based PSC cardiac

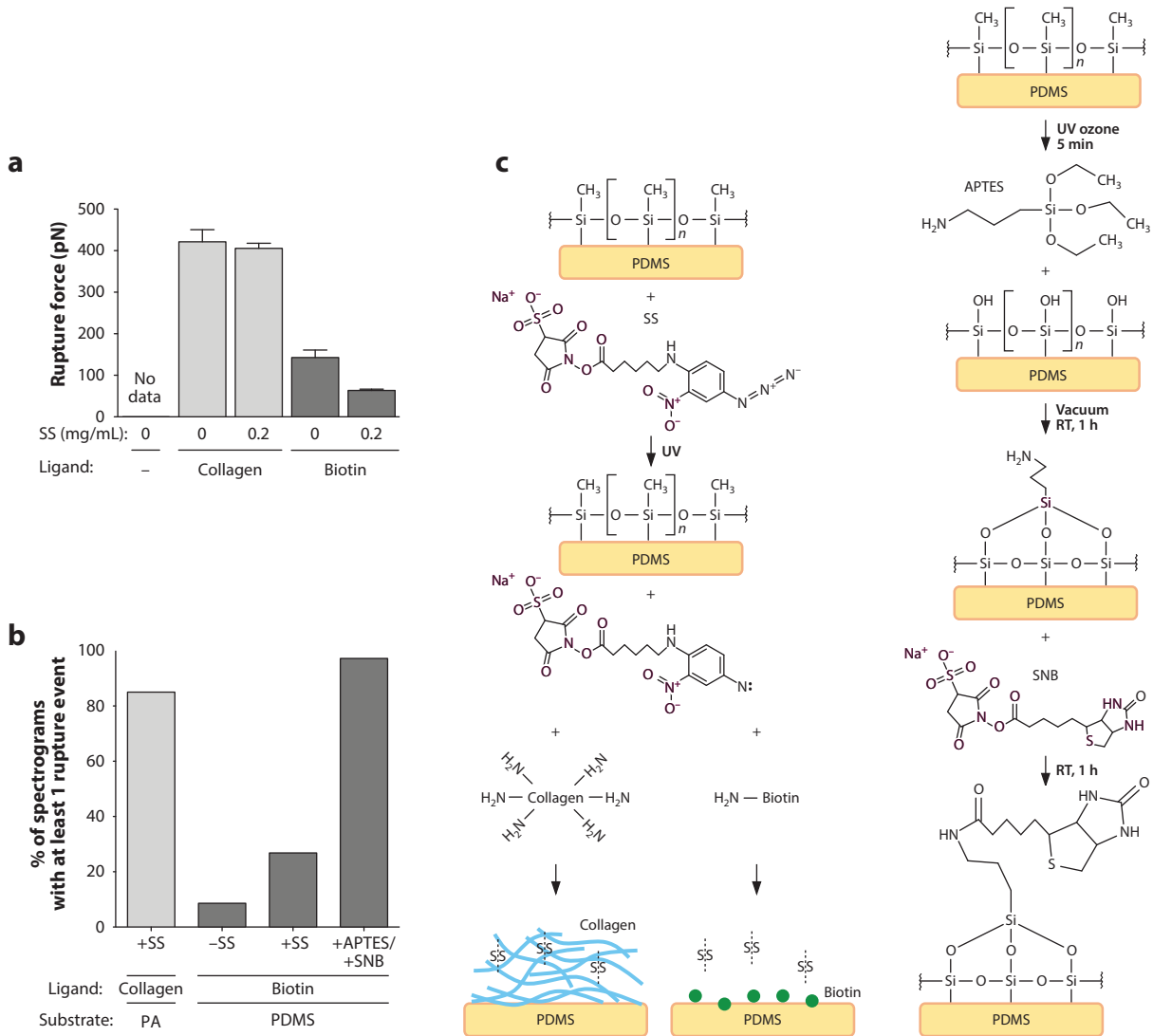


Figure 5

Characterization of the binding strength of the protein–substrate interface can be utilized to compare mechanobiology results across various cell–substrate interface platforms (e.g., PDMS versus PA hydrogel). (a) Functionalizing PDMS with or without sulfo-SANPAH (SS) does not change the rupture force suggesting collagen nonspecifically adsorbs to PDMS. (b) Different substrate and linker combinations lead to differences in binding strength of the protein–substrate interface. (c) Chemical groups and residues available at the substrate interface, linker, and ECM protein. Diagram for PDMS treated with SS and APTES/SNB linker. Abbreviations: APTES, (3-aminopropyl) triethoxysilane; ECM, extracellular matrix; NHS, *N*-hydroxysuccinimide; PA, polyacrylamide; PDMS, polydimethylsiloxane; RT, room temperature; SNB, sulfo-NHS-biotin; sulfo-SANPAH, sulfosuccinimidyl 6-(4'-azido-2'-nitrophenylamino)hexanoate; UV, ultraviolet. Figure adapted from Reference 99.

differentiation (129). Patel et al. (130) identified specific chemical moieties in three fully synthetic polymers, $C_2H_6N^+$ (amine), $C_5H_5O^+$ (furan ring), and $C_{10}H_{17}^+$ (isobornyl ring), that promoted greater PSC-CM adhesion and spread area. The synthetic polymers ionically interacted with the PSC-CMs.

Other studies showed that ligand composition can influence differentiation toward a specific cell lineage (9). Battista et al. (131) placed mouse PSCs within three-dimensional (3D) semi-interpenetrating polymer networks composed of collagen I and various amounts of fibronectin or laminin. Addition of laminin increased the PSCs' ability to differentiate into beating CMs, whereas addition of fibronectin stimulated endothelial cell differentiation. Jung et al. (132) utilized 1-kPa poly(ethylene glycol) (PEG) hydrogels to entrap murine PSCs and a mixture of ECM proteins. Using a design-of-experiments approach, these authors found that the optimal composition to induce in vitro cardiac differentiation without additional soluble factors was 61% collagen I, 24% laminin-111, and 15% fibronectin.

4.2. Stiffness

Matrix stiffness influences cell contractility, cytoskeleton structure, differentiation, and adhesion area (133, 134). During cardiac development, the stiffness of native myocardial tissue increases from 1 kPa at the embryo stage to 10–15 kPa at the adult stage (135, 136). After MI, the stiffness increases to 35–70 kPa (137). Substrate stiffness can alter CM contractility and cytoskeleton structure. By tuning PA hydrogel stiffness, Engler et al. (138) demonstrated that embryonic CMs on substrates with a physiologically relevant stiffness (11–17 kPa) promoted actomyosin striation and optimal work transfer to deform the substrate. However, embryonic CMs on stiffer substrates (34 kPa) had fewer myofibril striations, overstrained themselves, and stopped contracting, whereas embryonic CMs on softer substrates (1 kPa) contracted but did not transfer work to the substrate. Chung et al. (139) observed a temporal regulation of PSC-CMs' spontaneous contractility depending on the 3D hydrogel's cross-linking density (inherently varying stiffness). At the lowest cross-link density (0.45 kPa), the PSC-CMs began to spontaneously contract at day 1. In contrast, within the highest cross-link density (2.4 kPa), contraction was delayed until day 6. Hirata & Yamaoka (140) examined the role of substrate stiffness (9-, 20-, and 180-kPa PA hydrogels; tissue culture polystyrene) on mouse PSC cardiac differentiation. The cells on tissue culture plastic exhibited the highest expression of early cardiac differentiation marker genes. By contrast, the 20-kPa PA hydrogels showed the highest expression of cardiac contraction-related genes. These results suggest that a single culture substrate is not optimal for the various stages of cardiomyocyte differentiation. Kong et al. (141) demonstrated that substrate stiffness modulates indirect cardiac reprogramming of mouse embryonic fibroblasts. Mechanoresponsive signals (cell traction, cell area, Yes-associated protein) were able to predict cardiac reprogramming better than individual material properties (matrix modulus, ligand density, ligand type). Corbin et al. (134) developed a platform to instantaneously tune and reverse substrate stiffness (range 10–55 kPa) with magnetic fields. PSC-CMs seeded on soft and stiff substrates exhibited a small (2,600 μm^2) and a large (4,800 μm^2) spread area, respectively. The starlike shape of the PSC-CMs did not change with substrate stiffness.

4.3. Dimensionality: Two Versus Three Dimensions

Dimensionality can influence cell differentiation and degree of maturity. CMs natively exist within a 3D microenvironment. Branco et al. (142) demonstrated that cardiac differentiation of PSCs in a 3D microwell undergoes faster structural and functional maturation than in two-dimensional (2D) culture. Kerscher et al. (143) examined cardiac differentiation while PSCs maintained continuous 3D engagement with a PEG–fibrinogen hydrogel. Using the same small-molecule differentiation protocol, these authors found that 2D and 3D cultures showed similar differentiation efficiency, cardiac gene expression, and calcium handling. PSC-CMs within the 3D hydrogel

developed ultrastructural maturation, which was confirmed by the presence of transverse tubules on and after day 52. Zhang et al. (144) showed that PSC-CMs in a 3D microenvironment exhibited enhanced structural and functional maturation compared with 2D. Lemoine et al. (145) investigated differences in PSC-CM maturity within 2D and 3D cultures. PSC-CMs placed within a 3D microenvironment had upstroke velocities, morphology, and sodium current densities that were more physiologically relevant and similar to adult CMs in comparison to PSC-CMs in a 2D monolayer culture.

4.4. Topography

Topography can influence cell differentiation and maturation. The myocardial ECM contains a network of densely packed, aligned collagen I fibrils with an average diameter of 75 nm (66). Carson et al. (146) designed polyurethane acrylate nanoscale structures with various groove widths to probe the role of nanotopography. PSC-CM organization and structural maturation were controlled by nanogroove width in a biphasic manner. CM structural maturation indicators such as cell area, perimeter, alignment, circularity, and sarcomere length were improved using 700–1,000-nm widths. Seo et al. (147) observed CM differentiation promoted in multipotent mesodermal precursor cells on 200–280-nm-diameter polystyrene nanopillars. Abadi et al. (148) transferred primary human CM micro- and nanoscale topography features onto a PDMS substrate. The authors then showed that these submicrometer topographies on PDMS influence PSC-CMs' differentiation rate and maturity. Protein adsorption on PDMS is known to be influenced by topography; thus, special care must be taken to decouple properties such as protein density and topography (149).

5. SUMMARY AND FUTURE DIRECTIONS FOR CONTROLLING THE MICROENVIRONMENT OF CARDIOMYOCYTES VIA BIOMATERIALS

The goal of mimicking different components of the native cardiac microenvironment is to recapitulate the desired CM responses *in vitro*. Knowledge of what integrin types CMs use to natively interact with their microenvironment can be used to rationalize the design of specific binding sites in a biomaterial. Outside-in signaling allows the ECM to control integrin expression (150) and, thus, downstream mechanical signaling. Most *in vitro* CM mechanobiology platforms have focused on cell–ECM interactions, but opportunities exist to vary and probe the nature of the ligand and its attachment, as well as the role of cell–cell interactions. For example, myocardial tissue samples demonstrate the prevalence of intercalated discs whereby neighboring cells form physical and electrical connections. Connexin-43 and N-cadherin are, respectively, the most common gap junction protein and adherens junction protein expressed in CMs (28, 151). Studies of pairs of CMs on hydrogels found that the cell–cell interface transitioned from dominantly cell–ECM to cell–cell adhesion proteins over time (152). CMs on N-cadherin-coated PA hydrogel sustained forces similar to those of CMs on ECM-coated substrates, but they had different cytoskeleton architectures (153). CMs can also be mechanically coupled via underlying substrate deformations and can experience long-term modification after the mechanical stimulus is removed (154).

Current *in vitro* approaches lack temporal changes in the microenvironment's biochemical and biophysical properties that recapitulate heart development, and PSC-CMs exhibit properties of early to late fetal CMs (28). Thus, localized control of ligand type and placement, and of stiffness and cyclic stretch, would enable more precise studies of the variations and dynamics in the myocardium. Temporal and reversible control over biochemical and biophysical properties will better allow researchers to mimic heart changes in the microenvironment during development or

a disease state. An open question in the field is whether mimicking the evolution of the cardiac environment in vitro can increase the maturity and utility of PSC-CM models. More research is needed to control and tune specific biointerface properties; to quantify biomaterial and cell-adhesive properties; and to enable precision studies of the role of cardiac cell-ECM and cell-cell interactions in development, homeostasis, and disease.

DISCLOSURE STATEMENT

The authors are not aware of any affiliations, memberships, funding, or financial holdings that might be perceived as affecting the objectivity of this review.

ACKNOWLEDGMENTS

We thank current and past members of Professor Beth Pruitt's research group and Professor Sarah Heilshorn's research group for discussions and helpful comments on the manuscript. We also thank Dave Wallace for assistance with figure preparation. The writing of this review was supported by the American Heart Association (17CSA33590101); the National Science Foundation (CMMI 1662431, Graduate Research Fellowship Program); the National Academies of Science, Engineering, and Medicine (Ford Foundation Predoctoral Fellowship); and the National Institutes of Health (1R21GM131981-01, 5UG3TR002588-02, 1R21HL13099301).

LITERATURE CITED

1. Bowers SLK, McFadden WA, Borg TK, Baudino TA. 2012. Desmoplakin is important for proper cardiac cell-cell interactions. *Microsc. Microanal.* 18:107-14
2. Rienks M, Papageorgiou A-P, Frangogiannis NG, Heymans S. 2014. Myocardial extracellular matrix: an ever-changing and diverse entity. *Circ. Res.* 114:872-88
3. Simmons CS, Petzold BC, Pruitt BL. 2012. Microsystems for biomimetic stimulation of cardiac cells. *Lab Chip* 12:3235-48
4. Zak R. 1973. Cell proliferation during cardiac growth. *Am. J. Cardiol.* 31:211-19
5. Später D, Hansson EM, Zangi L, Chien KR. 2014. How to make a cardiomyocyte. *Development* 141:4418-31
6. De Franceschi N, Hamidi H, Alanko J, Sahgal P, Ivaskà J. 2015. Integrin traffic—the update. *J. Cell Sci.* 128:839-52
7. Frantz C, Stewart KM, Weaver VM. 2010. The extracellular matrix at a glance. *J. Cell Sci.* 123:4195-200
8. Hynes RO. 2009. The extracellular matrix: not just pretty fibrils. *Science* 326:1216-19
9. Israeli-Rosenberg S, Manso AM, Okada H, Ross RS. 2014. Integrins and integrin-associated proteins in the cardiac myocyte. *Circ. Res.* 114:572-86
10. Michele DE, Kabaeva Z, Davis SL, Weiss RM, Campbell KP. 2009. Dystroglycan matrix receptor function in cardiac myocytes is important for limiting activity-induced myocardial damage. *Circ. Res.* 105:984-93
11. Adams JC, Brancaccio A. 2015. The evolution of the dystroglycan complex, a major mediator of muscle integrity. *Biol. Open* 4:1163-79
12. Xie J, He G, Chen Q, Sun J, Dai Q, et al. 2016. Syndecan-4 signaling is required for exercise-induced cardiac hypertrophy. *Mol. Med.* 22:192-201
13. Peter AK, Cheng H, Ross RS, Knowlton KU, Chen J. 2011. The costamere bridges sarcomeres to the sarcolemma in striated muscle. *Prog. Pediatr. Cardiol.* 31:83-88
14. Samarel AM. 2005. Costameres, focal adhesions, and cardiomyocyte mechanotransduction. *Am. J. Physiol. Heart Circ. Physiol.* 298:H2291-301
15. Baldwin HS, Buck CA. 1994. Integrins and other cell adhesion molecules in cardiac development. *Trends Cardiovasc. Med.* 4:178-87

16. Forbes MS, Sperelakis N. 1985. Intercalated discs of mammalian heart: a review of structure and function. *Tissue Cell* 17:605–48
17. Ross RS, Borg TK. 2001. Integrins and the myocardium. *Circ. Res.* 88:1112–19
18. Huvencers S, Danen EHJ. 2009. Adhesion signaling—crosstalk between integrins, Src and Rho. *J. Cell Sci.* 122:1059–69
19. Humphries JD, Chastney MR, Askari JA, Humphries MJ. 2019. Signal transduction via integrin adhesion complexes. *Curr. Opin. Cell Biol.* 56:14–21
20. Lundgren E, Gullberg D, Rubin K, Borg TK, Terracio MJ, Terracio L. 1988. In vitro studies on adult cardiac myocytes: attachment and biosynthesis of collagen type IV and laminin. *J. Cell. Physiol.* 136:43–53
21. Mott JD, Werb Z. 2004. Regulation of matrix biology by matrix metalloproteinases. *Curr. Opin. Cell Biol.* 16:558–64
22. Miner EC, Miller WL. 2006. A look between the cardiomyocytes: the extracellular matrix in heart failure. *Mayo Clin. Proc.* 81:71–76
23. Mishra PK, Givvimani S, Chavali V, Tyagi SC. 2013. Cardiac matrix: a clue for future therapy. *Biochim. Biophys. Acta Mol. Basis Dis.* 1832:2271–76
24. Barczyk M, Carracedo S, Gullberg D. 2010. Integrins. *Cell Tissue Res.* 339:269–80
25. Takahashi K, Tanabe K, Ohnuki M, Narita M, Ichisaka T, et al. 2007. Induction of pluripotent stem cells from adult human fibroblasts by defined factors. *Cell* 131:861–72
26. Gherghiceanu M, Barad L, Novak A, Reiter I, Itskovitz-Eldor J, et al. 2011. Cardiomyocytes derived from human embryonic and induced pluripotent stem cells: comparative ultrastructure. *J. Cell. Mol. Med.* 15:2539–51
27. Yang X, Pabon L, Murry CE. 2014. Engineering adolescence: maturation of human pluripotent stem cell–derived cardiomyocytes. *Circ. Res.* 114:511–23
28. Scuderi GJ, Butcher J. 2017. Naturally engineered maturation of cardiomyocytes. *Front. Cell Dev. Biol.* 5:50
29. Milani-Nejad N, Janssen PML. 2014. Small and large animal models in cardiac contraction research: advantages and disadvantages. *Pharmacol. Ther.* 141:235–49
30. Spudich JA. 2014. Hypertrophic and dilated cardiomyopathy: Four decades of basic research on muscle lead to potential therapeutic approaches to these devastating genetic diseases. *Biophys. J.* 106:1236–49
31. Kolanowski TJ, Antos CL, Guan K. 2017. Making human cardiomyocytes up to date: derivation, maturation state and perspectives. *Int. J. Cardiol.* 241:379–86
32. Yang X, Pabon L, Murry CE. 2014. Engineering adolescence. *Circ. Res.* 114:511–23
33. Lundy SD, Zhu W-Z, Regnier M, Laflamme MA. 2013. Structural and functional maturation of cardiomyocytes derived from human pluripotent stem cells. *Stem Cells Dev.* 22:1991–2002
34. Ronaldson-Bouchard K, Ma SP, Yeager K, Chen T, Song L, et al. 2018. Advanced maturation of human cardiac tissue grown from pluripotent stem cells. *Nature* 556:239–43
35. Liu AP, Chaudhuri O, Parekh SH. 2017. New advances in probing cell–extracellular matrix interactions. *Integr. Biol.* 9:383–405
36. Darnell M, Mooney DJ. 2017. Leveraging advances in biology to design biomaterials. *Nat. Mater.* 16:1178–85
37. Campbell ID, Humphries MJ. 2011. Integrin structure, activation, and interactions. *Cold Spring Harb. Perspect. Biol.* 3:a004994
38. Humphries JD, Byron A, Humphries MJ. 2006. Integrin ligands at a glance. *J. Cell Sci.* 119:3901–3
39. Roca-Cusachs P, Gauthier NC, Del Rio A, Sheetz MP. 2009. Clustering of $\alpha_5\beta_1$ integrins determines adhesion strength whereas $\alpha_v\beta_3$ and talin enable mechanotransduction. *PNAS* 106:16245–50
40. Balcioglu HE, van Hoorn H, Donato DM, Schmidt T, Danen EHJ. 2015. The integrin expression profile modulates orientation and dynamics of force transmission at cell–matrix adhesions. *J. Cell Sci.* 128:1316–26
41. Kechagia JZ, Ivaska J, Roca-Cusachs P. 2019. Integrins as biomechanical sensors of the microenvironment. *Nat. Rev. Mol. Cell Biol.* 20:457–73
42. Vogel C, Marcotte EM. 2012. Insights into the regulation of protein abundance from proteomic and transcriptomic analyses. *Nat. Rev. Genet.* 13:227–32

43. Meliopoulos VA, Schultz-Cherry S. 2018. Although it's painful: the importance of stringent antibody validation. *PLOS Pathog.* 14:e1006701
44. Chen C, Li R, Ross RS, Manso AM. 2016. Integrins and integrin-related proteins in cardiac fibrosis. *J. Mol. Cell. Cardiol.* 93:162–74
45. Brancaccio M, Cabodi S, Belkin AM, Collo G, Koteliensky VE, et al. 1998. Differential onset of expression of alpha 7 and beta 1D integrins during mouse heart and skeletal muscle development. *Cell Adhes. Commun.* 5:193–205
46. Wiencierz AM, Kernbach M, Ecklebe J, Monnerat G, Tomiuk S, et al. 2015. Differential expression levels of integrin α_6 enable the selective identification and isolation of atrial and ventricular cardiomyocytes. *PLOS ONE* 10:e0143538
47. Humphries JD, Byron A, Humphries MJ. 2006. Integrin ligands at a glance. *J. Cell Sci.* 119:3901–3
48. Terracio L, Rubin K, Gullberg D, Balog E, Carver W, et al. 1991. Expression of collagen binding integrins during cardiac development and hypertrophy. *Circ. Res.* 68:734–44
49. Nawata J, Ohno I, Ioyama S, Suzuki J, Miura S, et al. 1999. Differential expression of α_1 , α_3 and α_5 integrin subunits in acute and chronic stages of myocardial infarction in rats. *Cardiovasc. Res.* 43:371–81
50. Domogatskaya A, Rodin S, Tryggvason K. 2012. Functional diversity of laminins. *Annu. Rev. Cell Dev. Biol.* 28:523–53
51. Babbitt CJ, Shai S-Y, Harpf AE, Pham CG, Ross RS. 2002. Modulation of integrins and integrin signaling molecules in the pressure-loaded murine ventricle. *Histochem. Cell Biol.* 118:431–39
52. Van Der Flier A, Gaspar AC, Thorsteinsdóttir S, Baudoin C, Groeneveld E, et al. 1997. Spatial and temporal expression of the β 1D integrin during mouse development. *Dev. Dyn.* 210:472–86
53. Belkin AM, Zhidkova NI, Balzac F, Altruda F, Tomatis D, et al. 1996. Beta 1D integrin displaces the beta 1A isoform in striated muscles: localization at junctional structures and signaling potential in nonmuscle cells. *J. Cell Biol.* 132:211–26
54. Sun M, Opavsky MA, Stewart DJ, Rabinovitch M, Dawood F, et al. 2003. Temporal response and localization of integrins β_1 and β_3 in the heart after myocardial infarction. *Circulation* 107:1046–52
55. Krishnamurthy P, Subramanian V, Singh M, Singh K. 2006. Deficiency of β_1 integrins results in increased myocardial dysfunction after myocardial infarction. *Heart* 92:1309–15
56. Ichikawa Y, Zemljic-Harpe AE, Zhang Z, McKirnan MD, Manso AM, et al. 2017. Modulation of caveolins, integrins and plasma membrane repair proteins in anthracycline-induced heart failure in rabbits. *PLOS ONE* 12:e0177660
57. Manso AM, Okada H, Sakamoto FM, Moreno E, Monkley SJ, et al. 2017. Loss of mouse cardiomyocyte talin-1 and talin-2 leads to β -1 integrin reduction, costameric instability, and dilated cardiomyopathy. *PNAS* 114:E6250–59
58. Schips TG, Vanhoutte D, Vo A, Correll RN, Brody MJ, et al. 2019. Thrombospondin-3 augments injury-induced cardiomyopathy by intracellular integrin inhibition and sarcolemmal instability. *Nat. Commun.* 10:76
59. Rowland TJ, Miller LM, Blaschke AJ, Doss EL, Bonham AJ, et al. 2010. Roles of integrins in human induced pluripotent stem cell growth on Matrigel and vitronectin. *Stem Cells Dev.* 19:1231–40
60. Ja KPMM, Miao Q, Zhen Tee NG, Lim SY, Nandihalli M, et al. 2016. iPSC-derived human cardiac progenitor cells improve ventricular remodelling via angiogenesis and interstitial networking of infarcted myocardium. *J. Cell. Mol. Med.* 20:323–32
61. Yu T, Miyagawa S, Miki K, Saito A, Fukushima S, et al. 2013. In vivo differentiation of induced pluripotent stem cell-derived cardiomyocytes. *Circ. J.* 77:1297–306
62. Karpievitch YV, Polpitiya AD, Anderson GA, Smith RD, Dabney AR. 2010. Liquid chromatography mass spectrometry-based proteomics: biological and technological aspects. *Ann. Appl. Stat.* 4:1797–823
63. Schmuck EG, Hematti P, Raval AN, eds. 2018. *Cardiac Extracellular Matrix Fundamental Science to Clinical Applications*. Cham, Switz.: Springer
64. Chang CW, Dalgliesh AJ, López JE, Griffiths LG. 2016. Cardiac extracellular matrix proteomics: challenges, techniques, and clinical implications. *Proteom. Clin. Appl.* 10:39–50
65. Schwach V, Passier R. 2019. Native cardiac environment and its impact on engineering cardiac tissue. *Biomater. Sci.* 7:3566–80

66. de Souza RR. 2002. Aging of myocardial collagen. *Biogerontology* 3:325–35
67. Bashey RI, Martinez-Hernandez A, Jimenez SA. 1992. Isolation, characterization, and localization of cardiac collagen type VI associations with other extracellular matrix components. *Circ. Res.* 70:1006–17
68. Fomovsky GM, Thomopoulos S, Holmes JW. 2010. Contribution of extracellular matrix to the mechanical properties of the heart. *J. Mol. Cell. Cardiol.* 48:490–96
69. Speiser B, Riess CF, Schaper J. 1991. The extracellular matrix in human myocardium. Part I: Collagens I, III, IV, and VI. *Cardioscience* 2:225–32
70. Hanson KP, Jung JP, Tran QA, Hsu S-PP, Iida R, et al. 2013. Spatial and temporal analysis of extracellular matrix proteins in the developing murine heart: a blueprint for regeneration. *Tissue Eng. A* 19:1132–43
71. Marjjanowski MMH, van der Loos CM, Mohrschladt MF, Becker AE. 1994. The neonatal heart has a relatively high content of total collagen and type I collagen, a condition that may explain the less compliant state. *J. Am. Coll. Cardiol.* 23:1204–8
72. Borg TK, Gay RE, Johnson LD. 1982. Changes in the distribution of fibronectin and collagen during development of the neonatal rat heart. *Coll. Relat. Res.* 2:211–18
73. Gershlak JR, Resnikoff JL, Sullivan KE, Williams C, Wang RM, Black LD III. 2013. Mesenchymal stem cells ability to generate traction stress in response to substrate stiffness is modulated by the changing extracellular matrix composition of the heart during development. *Biochem. Biophys. Res. Commun.* 439:161–66
74. Williams C, Quinn KP, Georgakoudi I, Black LD III. 2014. Young developmental age cardiac extracellular matrix promotes the expansion of neonatal cardiomyocytes in vitro. *Acta Biomater.* 10:194–204
75. Wei S, Chow LTC, Shum IOL, Qin L, Sanderson JE. 1999. Left and right ventricular collagen type I/III ratios and remodeling post-myocardial infarction. *J. Card. Fail.* 5:117–26
76. Sullivan KE, Quinn KP, Tang KM, Georgakoudi I, Black LD III. 2014. Extracellular matrix remodeling following myocardial infarction influences the therapeutic potential of mesenchymal stem cells. *Stem Cell Res. Ther.* 5:14
77. Quinn KP, Sullivan KE, Liu Z, Ballard Z, Siokatas C, et al. 2016. Optical metrics of the extracellular matrix predict compositional and mechanical changes after myocardial infarction. *Sci. Rep.* 6:35823
78. Yang H, Borg TK, Liu H, Gao BZ. 2015. Interactive relationship between basement-membrane development and sarcomerogenesis in single cardiomyocytes. *Exp. Cell Res.* 330:222–32
79. Luther DJ, Thodeti CK, Shamhart PE, Adapala RK, Hodnichak C, et al. 2012. Absence of type VI collagen paradoxically improves cardiac function, structure, and remodeling after myocardial infarction. *Circ. Res.* 110:851–56
80. Rasi K, Piuholta J, Czabanka M, Sormunen R, Ilves M, et al. 2010. Collagen XV is necessary for modeling of the extracellular matrix and its deficiency predisposes to cardiomyopathy. *Circ. Res.* 107:1241–52
81. Jourdan-LeSaux C, Zhang J, Lindsey ML. 2010. Extracellular matrix roles during cardiac repair. *Life Sci.* 87:391–400
82. Boateng SY, Lateef SS, Mosley W, Hartman TJ, Hanley L, Russell B. 2005. RGD and YIGSR synthetic peptides facilitate cellular adhesion identical to that of laminin and fibronectin but alter the physiology of neonatal cardiac myocytes. *Am. J. Physiol. Cell Physiol.* 288:C30–38
83. Roediger M, Miosge N, Gersdorff N. 2010. Tissue distribution of the laminin β 1 and β 2 chain during embryonic and fetal human development. *J. Mol. Histol.* 41:177–84
84. Yap L, Wang J-W, Moreno-Moral A, Chong LY, Sun Y, et al. 2019. *In vivo* generation of post-infarct human cardiac muscle by laminin-promoted cardiovascular progenitors. *Cell Rep.* 26:3231–45
85. Ulrich MMW, Janssen AMH, Daemen MJAP, Rappaport L, Samuel J-L, et al. 1997. Increased expression of fibronectin isoforms after myocardial infarction in rats. *J. Mol. Cell Cardiol.* 29:2533–43
86. Linask KK, Lash JW. 1988. A role for fibronectin in the migration of avian precardiac cells. II. Rotation of the heart-forming region during different stages and its effects. *Dev. Biol.* 129:324–29
87. van Dijk A, Niessen HWM, Ursem W, Twisk JWR, Visser FC, van Milligen FJ. 2008. Accumulation of fibronectin in the heart after myocardial infarction: a putative stimulator of adhesion and proliferation of adipose-derived stem cells. *Cell Tissue Res.* 332:289–98

88. Balasubramanian S, Quinones L, Kasiganesan H, Zhang Y, Pleasant DL. 2012. $\beta 3$ integrin in cardiac fibroblast is critical for extracellular matrix accumulation during pressure overload hypertrophy in mouse. *PLOS ONE* 7:e45076
89. Ramos IT, Henningsson M, Nezafat M, Lavin B, Lorrio S, et al. 2018. Simultaneous assessment of cardiac inflammation and extracellular matrix remodeling after myocardial infarction. *Circ. Cardiovasc. Imaging* 11:e007453
90. Lee JP, Kassianidou E, MacDonald JI, Francis MB, Kumar S. 2016. N-terminal specific conjugation of extracellular matrix proteins to 2-pyridinecarboxaldehyde functionalized polyacrylamide hydrogels. *Biomaterials* 102:268–76
91. Halldorsson S, Lucumi E, Gómez-Sjöberg R, Fleming RMT. 2015. Advantages and challenges of microfluidic cell culture in polydimethylsiloxane devices. *Biosens. Bioelectron.* 63:218–31
92. Damljanović V, Lagerholm BC, Jacobson K. 2005. Bulk and micropatterned conjugation of extracellular matrix proteins to characterized polyacrylamide substrates for cell mechanotransduction assays. *Biotechniques* 39:847–51
93. Nelson CM, Raghavan S, Tan JL, Chen CS. 2003. Degradation of micropatterned surfaces by cell-dependent and -independent processes. *Langmuir* 19:1493–99
94. Tang X, Yakut Ali M, Saif MTA. 2012. A novel technique for micro-patterning proteins and cells on polyacrylamide gels. *Soft Matter* 8:7197–206
95. Moeller J, Denisin AK, Sim JY, Wilson RE, Ribeiro AJS, Pruitt BL. 2018. Controlling cell shape on hydrogels using lift-off protein patterning. *PLOS ONE* 13:e0189901
96. Ribeiro AJS, Denisin AK, Wilson RE, Pruitt BL. 2016. For whom the cells pull: hydrogel and micropost devices for measuring traction forces. *Methods* 94:51–64
97. Pelham RJ, Wang Y-L. 1997. Cell locomotion and focal adhesions are regulated by substrate flexibility. *PNAS* 94:13661–65
98. Lekka M, Pabijan J, Orzechowska B. 2019. Morphological and mechanical stability of bladder cancer cells in response to substrate rigidity. *Biochim. Biophys. Acta Gen. Subj.* 1863:1006–14
99. Wen JH, Vincent LG, Fuhrmann A, Choi YS, Hribar K, et al. 2014. Interplay of matrix stiffness and protein tethering in stem cell differentiation. *Nat. Mater.* 13:979–87
100. Dembo M, Wang YL. 1999. Stresses at the cell-to-substrate interface during locomotion of fibroblasts. *Biophys. J.* 76:2307–16
101. Charrier EE, Pogoda K, Wells RG, Janmey PA. 2018. Control of cell morphology and differentiation by substrates with independently tunable elasticity and viscous dissipation. *Nat. Commun.* 9:449
102. Reinhart-King CA, Dembo M, Hammer DA. 2005. The dynamics and mechanics of endothelial cell spreading. *Biophys. J.* 89:676–89
103. Macdonald JI, Munch HK, Moore T, Francis MB. 2015. One-step site-specific modification of native proteins with 2-pyridinecarboxyaldehydes. *Nat. Chem. Biol.* 11:326–31
104. Gokaltun A, Yarmush ML, Asatekin A, Usta OB. 2017. Recent advances in nonbiofouling PDMS surface modification strategies applicable to microfluidic technology. *Technology* 5:1–12
105. Khnouf R, Karasneh D, Albiss BA. 2016. Protein immobilization on the surface of polydimethylsiloxane and polymethyl methacrylate microfluidic devices. *Electrophoresis* 37:529–35
106. De Silva MN, Desai R, Odde DJ. 2004. Micro-patterning of animal cells on PDMS substrates in the presence of serum without use of adhesion inhibitors. *Biomed. Microdevices* 6:219–22
107. Eteshola E, Leckband D. 2001. Development and characterization of an ELISA assay in PDMS microfluidic channels. *Sens. Actuators B* 72:129–33
108. Mobasser SA, Zijl S, Salameti V, Walko G, Stannard A, et al. 2019. Patterning of human epidermal stem cells on undulating elastomer substrates reflects differences in cell stiffness. *Acta Biomater.* 87:256–64
109. Kim Y, Kwon C, Jeon H. 2017. Genetically engineered phage induced selective H9c2 cardiomyocytes patterning in PDMS microgrooves. *Materials* 10:E973
110. Ferguson GS, Chaudhury MK, Biebuyck HA, Whitesides GM. 1993. Monolayers on disordered substrates: self-assembly of alkyltrichlorosilanes on surface-modified polyethylene and poly(dimethylsiloxane). *Macromolecules* 26:5870–75

111. Chaudhury MK, Whitesides GM. 1991. Direct measurement of interfacial interactions between semi-spherical lenses and flat sheets of poly(dimethylsiloxane) and their chemical derivatives. *Langmuir* 7:1013–25
112. Zhang W, Choi DS, Nguyen YH, Chang J, Qin L. 2013. Studying cancer stem cell dynamics on PDMS surfaces for microfluidics device design. *Sci. Rep.* 3:2332
113. Yang Y, Kulangara K, Lam RTS, Dharmawan R, Leong KW. 2012. Effects of topographical and mechanical property alterations induced by oxygen plasma modification on stem cell behavior. *ACS Nano* 6:8591–98
114. Nam KH, Jamilpour N, Mfoumou E, Wang FY, Zhang DD, Wong PK. 2014. Probing mechanoregulation of neuronal differentiation by plasma lithography patterned elastomeric substrates. *Sci. Rep.* 4:6965
115. Farrell M, Beaudoin S. 2010. Surface forces and protein adsorption on dextran- and polyethylene glycol-modified polydimethylsiloxane. *Colloids Surfaces B* 81:468–75
116. Hu S, Chen TH, Zhao Y, Wang Z, Lam RHW. 2018. Protein–substrate adhesion in microcontact printing regulates cell behavior. *Langmuir* 34:1750–59
117. Kuddannaya S, Chuah YJ, Lee MHA, Menon NV, Kang Y, Zhang Y. 2013. Surface chemical modification of poly(dimethylsiloxane) for the enhanced adhesion and proliferation of mesenchymal stem cells. *ACS Appl. Mater. Interfaces* 5:9777–84
118. Leivo J, Kartasalo K, Kallio P, Virjula S, Miettinen S, et al. 2017. A durable and biocompatible ascorbic acid-based covalent coating method of polydimethylsiloxane for dynamic cell culture. *J. R. Soc. Interface* 14:20170318
119. Huang B, Wu H, Kim S, Kobilka BK, Zare RN. 2006. Phospholipid biotinylation of polydimethylsiloxane (PDMS) for protein immobilization. *Lab Chip* 6:369–73
120. Wang RM, Christman KL. 2016. Decellularized myocardial matrix hydrogels: in basic research and preclinical studies. *Adv. Drug Deliv. Rev.* 96:77–82
121. Santoro R, Perrucci GL, Gowran A, Pompilio G. 2019. Unchain my heart: integrins at the basis of iPSC cardiomyocyte differentiation. *Stem Cells Int.* 2019:1–20
122. Bejleri D, Davis ME. 2019. Decellularized extracellular matrix materials for cardiac repair and regeneration. *Adv. Healthc. Mater.* 8:1801217
123. Taylor DA, Parikh RB, Sampaio LC. 2017. Bioengineering hearts: simple yet complex. *Curr. Stem Cell Rep.* 3:35–44
124. Paoletti C, Divieto C, Chiono V. 2018. Impact of biomaterials on differentiation and reprogramming approaches for the generation of functional cardiomyocytes. *Cells* 7:E114
125. Chen QZ, Harding SE, Ali NN, Lyon AR, Boccaccini AR. 2008. Biomaterials in cardiac tissue engineering: ten years of research survey. *Mater. Sci. Eng. R* 59:1–37
126. Segers VFM, Lee RT. 2011. Biomaterials to enhance stem cell function in the heart. *Circ. Res.* 109:910–22
127. Borg TK, Rubin K, Lundgren E, Borg K, Öbrink B. 1984. Recognition of extracellular matrix components by neonatal and adult cardiac myocytes. *Dev. Biol.* 104:86–96
128. Burridge PW, Matsa E, Shukla P, Lin ZC, Churko JM, et al. 2014. Chemically defined generation of human cardiomyocytes. *Nat. Methods* 11:855–60
129. Hirata N, Nakagawa M, Fujibayashi Y, Yamauchi K, Murata A, et al. 2014. A chemical probe that labels human pluripotent stem cells. *Cell Rep.* 6:1165–74
130. Patel AK, Celiz AD, Rajamohan D, Anderson DG, Langer R, et al. 2015. A defined synthetic substrate for serum-free culture of human stem cell derived cardiomyocytes with improved functional maturity identified using combinatorial materials microarrays. *Biomaterials* 61:257–65
131. Battista S, Guarnieri D, Borselli C, Zeppetelli S, Borzacchiello A, et al. 2005. The effect of matrix composition of 3D constructs on embryonic stem cell differentiation. *Biomaterials* 26:6194–207
132. Jung JP, Hu D, Domian IJ, Ogle BM. 2015. An integrated statistical model for enhanced murine cardiomyocyte differentiation via optimized engagement of 3D extracellular matrices. *Sci. Rep.* 5:18705
133. Discher DE, Janmey P, Wang Y. 2005. Tissue cells feel and respond to the stiffness of their substrate. *Science* 310:1139–43

134. Corbin EA, Vite A, Peyster EG, Bhoopalam M, Brandimarto J, et al. 2019. Tunable and reversible substrate stiffness reveals a dynamic mechanosensitivity of cardiomyocytes. *ACS Appl. Mater. Interfaces* 11:20603–14
135. Young JL, Engler AJ. 2011. Hydrogels with time-dependent material properties enhance cardiomyocyte differentiation in vitro. *Biomaterials* 32:1002–9
136. Majkut S, Idema T, Swift J, Krieger C, Liu A, Discher DE. 2013. Heart-specific stiffening in early embryos parallels matrix and myosin expression to optimize beating. *Curr. Biol.* 23:2434–39
137. Berry MF, Engler AJ, Woo YJ, Pirolli TJ, Bish LT, et al. 2006. Mesenchymal stem cell injection after myocardial infarction improves myocardial compliance. *Am. J. Physiol. Heart Circ. Physiol.* 290:H2196–203
138. Engler AJ, Carag-Krieger C, Johnson CP, Raab M, Tang H-Y, et al. 2008. Embryonic cardiomyocytes beat best on a matrix with heart-like elasticity: Scar-like rigidity inhibits beating. *J. Cell Sci.* 121:3794–802
139. Chung C, Anderson E, Pera RR, Pruitt BL, Heilshorn SC. 2012. Hydrogel crosslinking density regulates temporal contractility of human embryonic stem cell-derived cardiomyocytes in 3D cultures. *Soft Matter*. 8:10141–48
140. Hirata M, Yamaoka T. 2018. Effect of stem cell niche elasticity/ECM protein on the self-beating cardiomyocyte differentiation of induced pluripotent stem (iPS) cells at different stages. *Acta Biomater.* 65:44–52
141. Kong YP, Rioja AY, Xue X, Sun Y, Fu J, Putnam AJ. 2018. A systems mechanobiology model to predict cardiac reprogramming outcomes on different biomaterials. *Biomaterials* 181:280–92
142. Branco MA, Cotovio JP, Rodrigues CAV, Vaz SH, Fernandes TG, et al. 2019. Transcriptomic analysis of 3D cardiac differentiation of human induced pluripotent stem cells reveals faster cardiomyocyte maturation compared to 2D culture. *Sci. Rep.* 9:9229
143. Kerscher P, Turnbull IC, Hodge AJ, Kim J, Seliktar D, et al. 2016. Direct hydrogel encapsulation of pluripotent stem cells enables ontomimetic differentiation and growth of engineered human heart tissues. *Biomaterials* 83:383–95
144. Zhang D, Shadrin IY, Lam J, Xian HQ, Snodgrass HR, Bursac N. 2013. Tissue-engineered cardiac patch for advanced functional maturation of human ESC-derived cardiomyocytes. *Biomaterials* 34:5813–20
145. Lemoine MD, Mannhardt I, Breckwoldt K, Prondzynski M, Flenner F, et al. 2017. Human iPSC-derived cardiomyocytes cultured in 3D engineered heart tissue show physiological upstroke velocity and sodium current density. *Sci. Rep.* 7:5464
146. Carson D, Hnilova M, Yang X, Nemeth CL, Tsui JH, et al. 2016. Nanotopography-induced structural anisotropy and sarcomere development in human cardiomyocytes derived from induced pluripotent stem cells. *ACS Appl. Mater. Interfaces* 8:21923–32
147. Seo HR, Joo HJ, Kim DH, Cui LH, Choi SC, et al. 2017. Nanopillar surface topology promotes cardiomyocyte differentiation through cofilin-mediated cytoskeleton rearrangement. *ACS Appl. Mater. Interfaces* 9:16803–12
148. Abadi PPSS, Garbern JC, Behzadi S, Hill MJ, Tresback JS, et al. 2018. Engineering of mature human induced pluripotent stem cell-derived cardiomyocytes using substrates with multiscale topography. *Adv. Funct. Mater.* 28:1–11
149. Chen H, Song W, Zhou F, Wu Z, Huang H, et al. 2009. The effect of surface microtopography of poly(dimethylsiloxane) on protein adsorption, platelet and cell adhesion. *Colloids Surf. B* 71:275–81
150. Delcommenne M, Streuli CH. 1995. Control of integrin expression by extracellular matrix. *J. Biol. Chem.* 270:26794–801
151. Vite A, Radice GL. 2014. N-Cadherin/catenin complex as a master regulator of intercalated disc function. *Cell Commun. Adhes.* 21:169–79
152. McCain ML, Lee H, Aratyn-Schaus Y, Kléber AG, Parker KK. 2012. Cooperative coupling of cell-matrix and cell-cell adhesions in cardiac muscle. *PNAS* 109:9881–86
153. Chopra A, Tabdanov E, Patel H, Janmey PA, Kresh JY. 2011. Cardiac myocyte remodeling mediated by N-cadherin-dependent mechanosensing. *Am. J. Physiol. Heart Circ. Physiol.* 300:H1252–66

154. Nitsan I, Drori S, Lewis YE, Cohen S, Tzliil S. 2016. Mechanical communication in cardiac cell synchronized beating. *Nat. Phys.* 12:472–77
155. Marsico G, Russo L, Quondamatteo F, Pandit A. 2018. Glycosylation and integrin regulation in cancer. *Trends Cancer* 4:537–52
156. Seetharaman S, Etienne-Manneville S. 2018. Integrin diversity brings specificity in mechanotransduction. *Biol. Cell* 110:49–64
157. Berk BC, Fujiwara K, Lehoux S. 2007. ECM remodeling in hypertensive heart disease. *J. Clin. Investig.* 117:568–75